Lunette dunes of Lake Torrens and their significance as paleoenvironmental indicators

Thesis submitted in accordance with the requirements of the University of Adelaide for an Honours Degree in Geology/Geophysics

Benjamin Andrew Koch

November 2016

THE UNIVERSITY
of ADELAIDE

LUNETTE DUNES OF LAKE TORRENS AND THEIR SIGNIFICANCE AS PALEOENVIRONMENTAL INDICATORS

LUNETTE DUNES OF LAKE TORRENS

ABSTRACT

This paper aims to provide an understanding of the variability of the lake level at Lake Torrens and use this as a proxy for climate throughout the last 50,000 thousand years (ka). Australia's climate has evolved throughout the Quaternary, with the Holocene experiencing much more variable episodes of wetness, however questions remain due to most previous works focused on different climatic regimes. Dunes characteristic of high clay content, known as lunettes, form adjacent to dry lakes in unique environmental settings and therefore can offer important information of lake hydrological phases. These dunes are useful climatic indicators as they form in response to prevailing winds during the middle to latter part of the dry season after water table lowering has occurred. A complex lunette system has formed on the eastern margin of Lake Torrens which has been found to record paleoenvironmental indicators through its mineralogical, textural and morphological characteristics. This study analysed this lunette system through mapping of surficial geomorphology and construction of a digitally elevated modal based on aerial photometry, sediment characterization for grain size, elemental and mineralogical composition and dating by optically stimulated luminescence (OSL). The key results suggest that the formation of two lunette units, indicating variable lake levels. These clay rich units were dated at ~40 ka and ~20 ka which agree with lake levels found from neighbouring Lake Frome. These results offer new insights and understanding of the climate variability in southern arid Australia, with significance for interpreting the mechanisms of multi-millennial climate change and associated hydrological response in the southern hemisphere arid continents.

KEYWORDS

Climate, clay, lunette, Australia, Lake Torrens

TABLE OF CONTENTS

LIST OF FIGURES AND TABLES

INTRODUCTION

Past studies conducted on the climatic variability of the Australian interior is very significant and important in understanding the nature of climate variability. However there are still many questions remaining about Australian climate during the Quaternary. Studies has already been undertaken on a range of Australian arid/semi-arid lakes including Lake Frome (J. M. Bowler, 1986), Lake Gregory (Veth et al., 2009), Lake Mungo (James M. Bowler et al., 2003; J. M. Bowler & Price, 1998) and Lake Eyre (Magee, Miller, Spooner, & Questiaux, 2004) describing the climatic regimes of which the lakes are situated, however Lake Torrens offers information more focused on the arid to semi-arid boundary which cannot be reliably analysed by other lakes.

Lunettes situated on the shorelines of ephemeral inland lakes can be used as key climatic indicators offering insight into wet and dry phases experienced by the lake (J. M. Bowler, 1981). Lunettes in southern South Australia are low crescentic stationary ridges which commonly occur on the eastern side of ephemeral lakes. There are two common types of lunettes; those composed predominantly of sand and those consisting of sands, silts and clays (Campbell, 1968). The size of these structures can vary from small to 50-60 metres in elevation (Bourne & Twidale, 2010). This creates an obstacle for air flow causing deflection and turbulence, which in turn leads to deposition on the lee side of a topographic barrier which merges downwind to form the linear sand ridges or dunes that dominate shorelines.

As climatic indicators lunettes can create relevant records dating back thousands of years of 'wet' and 'dry' phases of the ephemeral lakes they surround. With these ephemeral inland lakes having access to large catchment areas, an accurate precipitation/evaporation record of the region can be documented (De Deckker, 1983). Lake filling/drying histories

are then able to be created through the interpretation of lithological units found within lunette stratigraphy, with clay-rich layers typically diagnostic with drying periods and clay-poor layers diagnostic of wet periods.

Throughout the late Holocene, southern central Australia experienced a period of increased hydrologic activity was experienced (Gliganic et al., 2014) with the formation of calcareous soil (Motpena paleosol), possibly associated with warmer subhumid conditions between 16 and 12 kyr BP (Williams, 1973). The Lake Frome lunette provides a sensitive indicator of precipitation in a region with few robust terrestrial climate records. Lake Frome (Figure 1b) experienced a 'wet' phase at 13.2 ±0.8 kyr compared to 0-1 metre depth range experienced with current day conditions. Similar lakes in other parts of Australia such as Lake Mungo have experienced significant oscillations in lake level since human arrival 45 kyr further reiterating the constant changing of the climatic regime (Fitzsimmons, Stern, & Murray-Wallace, 2014). The creation of these paleosols has been interpreted as reflecting the region experiencing a temperate system with an increase in mean annual rainfall. Meanwhile, periods of fan building and lunette forming on the eastern side of the lake has been interpreted as an arid phase with occasional periods of flooding and a high water table.

This study will test the hypothesis that Lake Torrens experienced wet and dry periods similar to that of Lake Frome.

To address this hypothesis, this study aims to (1) characterise the late Quaternary lunette sediments at Lake Torrens (2) investigate which climatic regime Lake Torrens is influenced by comparing lake level curves with those found from Lake Frome and Lake Eyre and global sea level curves to see if there are any connections with global processes occurring.

The significance of understanding the timing, factors and controls for climate variability of inland Australia is that this could provide a vital piece of information to answer much larger questions such as 'Why does it rain in Australia?' or 'What is the future for Australia's climate under projected future scenarios?'.

GEOLOGICAL SETTING/BACKGROUND

Lake Torrens (Figure 1a) is found in a depression which has origins from the subsidence along the Torrens Fault or Lineament occurring during the early Eocene or Late Cretaceous. The Lake Torrens region has experienced times of sediment depocentre along the Arcoona Plateau and the Flinders Ranges.
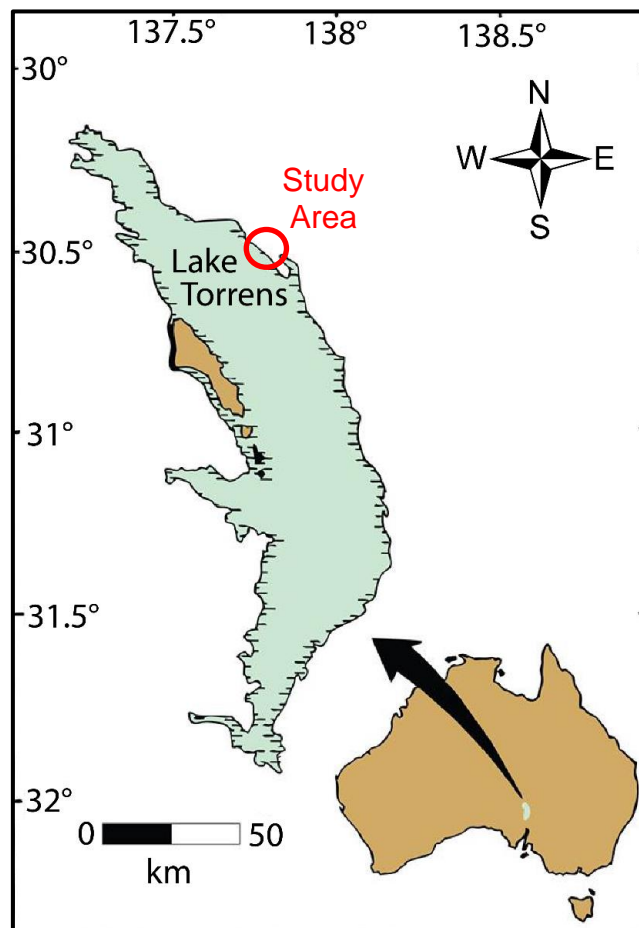
Figure 1a A map (which has been modified from Williams et al. (1998)) showing the location of Lake Torrens.

The upper surface of Lake Torrens consists of gypsum and halite, with a bed of gypsum 12 metres thick observed 5 kilometres from the eastern shoreline (Bourne and Twidale 2010). Alluvial fan building commenced approximately 30,000 kyr with the deposition of the Pooraka Formation which was followed by the soil formation occurring around 24,000 kyr (Wilkatana paleosol) (Johns, 1968). Alluvial fans found within the Flinders Ranges region can be observed adjacent to catchments uplifted by young (Pliocene-Quaternary) reverse faulting. This suggests that tectonic activity has created a control on the sediment accumulation rates along the ranges (Quigley, Sandiford, & Cupper, 2007). Early research by Williams (1973) has suggested that at 16,000 kyr the gypseous lunettes bordering the eastern shoreline (Lake Torrens Formation) were deposited. The lake is very shallow with a mean depth of 0.5 m when full and maximum depths of 1.5 m.
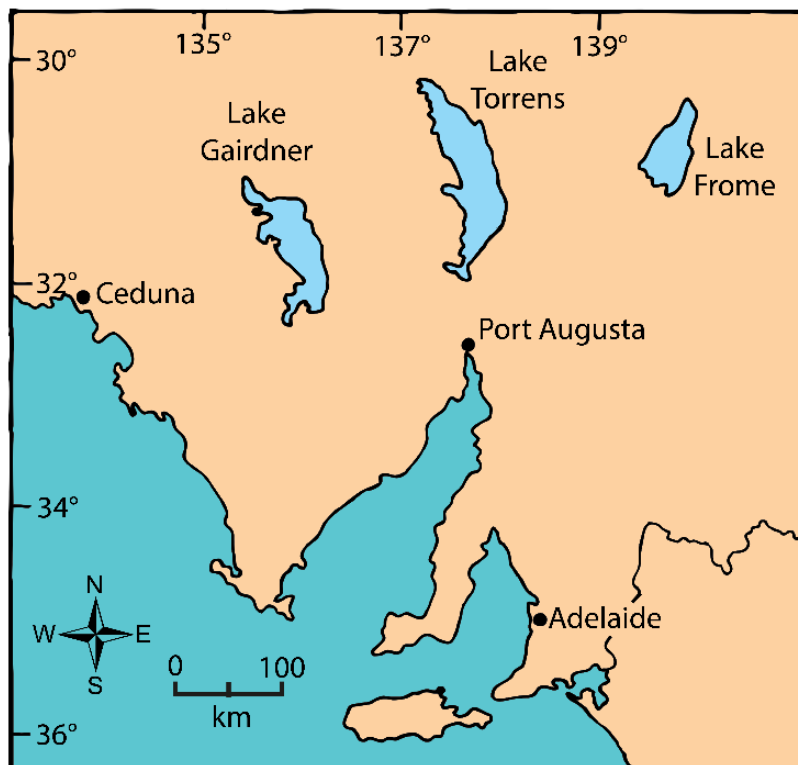
Figure 1b Displays the spatial relationship of inland lakes in South Australia adapted from (Schmid, 1990).

There are two ruling precipitation regimes which can affect central Australia; the Indo-Australian summer monsoon, and the front and depressions associated with the mid-latitude westerlies (Cohen et al., 2012). The monsoonal regime is the principal source of precipitation for Lake Eyre as runoff is captured by Australia's largest endoreic drainage system, however Lake Torrens, ~100 km to the south, receives most of its rainfall from the Southern Westerlies during winter months.
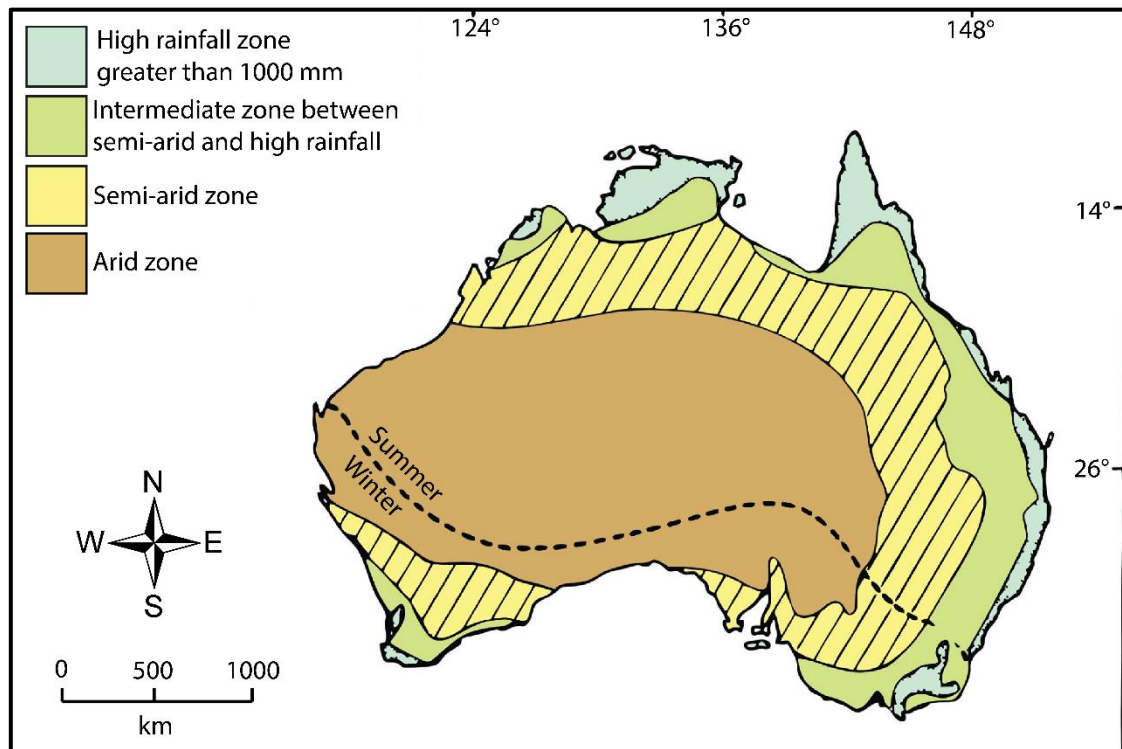
Figure 2 A modified map of the climatic regimes of Australia originally compiled by De Dekker (1983). Note the line which denotes the summer-winter rainfall boundary.

The mean annual rainfall of the Lake Torrens region is approximately 200 mm and falls within the arid area of Australia (figure 2). Average maximum air temperature is 34°C, with maxima above 40°C during summer, and average minimum temperature is approximately 4°C, with minima near 1°C in winter. The mean annual pan evaporation is approximately three metres (Williams, De Deckker, & Shiel, 1998).

METHODS

A variety of methods was utilised to address the research question and approached in stages. Pre-field work consisted of analysis of remote sensing data to identify suitable field sites, e.g. ArcGIS mapping. Once in the field, Stage 1 involved the collection of aerial photogrammetry data of the area and provided a high definition 3-dimensional model of the study area and enabled mapping of the surface stratigraphy. The second stage was soil sample collection from three strategically placed pits throughout the lunette system. An interpretation of wet or dry climates was interpreted through elemental, mineralogical and grain size analysis of these grains. Finally, the third stage was the OSL dating samples collected from the same pits to constrain the timing of events within the stratigraphic record. For further detail on methods used in this study please refer to the extended methods section in the appendix.

Air Photo Mapping

High-resolution photos of the study area were captured with 80% overlap using an E384 UAV on two pre-programmed missions at 50 and 70-metre altitude. Positioning was provided for ground targets using a CHC X90+ static GPS with 70-minute occupations post-processed with the AUSPOS service to achieve ~2 cm x, y and z-positioning. These images were processed to create an orthophoto and digital elevation model with a pixel resolution of approximately 5 cm with Agisoft Photoscan Professional and exported to ArcMap.

Field sediment logging and sampling

Three pits were dug throughout the lunette sequence in order to log the sediments and gauge an understanding of the distribution of grain sizes with depth. Samples were collected every 5 cm interval unless a stratigraphic unit boundary was encountered within

that 5 cm, in which case the sample range was altered to preserve the boundary. A total of 94 samples, each weighing approximately 300 grams were collected. Once collected, the samples were transported in Ziploc bags and stored under lab room conditions until analysis.

Grain Size Analysis

In the laboratory, samples were then loaded into an alfoil tray and placed in a 50ºC oven for a total of 48 hours to remove all moisture still present. They were then sieved to remove any grains larger than 1 mm in diameter, with the amount of larger size fraction recorded and stored separately. The remaining less than 1 mm sample was then analysed using a Mastersizer 2000 to estimate grain distributions as a percentage of the total sample, as per McDowell et al. (2013).

Gravimetric settling analysis was also performed as a reassurance of the grain size distribution throughout the three pits which is based upon the rate of different particle sizes settling out of suspension (Clifton, McDonald, Plater, & Oldfield, 1999). Samples were chosen by the sample range they were found in given by Table 1, as well as the samples already chosen to undergo clay separation XRD. The experiment was then carried out as per Tsao et al. (2013) for each sample.

Table 1

Sample	Pit 1	Sample	Pit 2	Sample	Pit 3
1.1	0-10cm	2.1	0-5cm	3.1	0-92cm
1.2	10-55cm	2.2	5-38cm	3.2	92-110cm
1.3	55-93cm	2.3	38-57cm	3.3	110-125cm
1.4	93-105cm	2.4	57-77cm	3.4	125-145cm
		2.5	77-110cm	3.5	145-164cm
		2.6	110-170cm		

X-Ray Fluorescence

An Olympus X-5000 Unites Laboratory EDXRF portable X-ray fluorescence scanner was used to obtain an elemental distribution throughout the samples from the three pits. This device was limited to observing elements heavier than magnesium and subject to detection level requirements for each element, once an element was encountered below detection it was recorded as a zero reading. Powdered samples were compacted into a circular mould and analysed for two minutes. The standards used were:

1947175 (clay and sand)

OREAS 901 (argillaceous sandstone)

1933084 (carbonate)

X-Ray Diffraction

All samples were analysed using x-ray diffraction in to identify the mineralogical composition of the sediments. All samples were crushed to a powder, loaded so that the grains were aligned randomly and analysed by a Bruker D8 Advance X-ray diffractometer with a copper source, scanning between a 2θ range of 3.5° and 45° with a step size of 0.05° at 1.5 seconds a step. The data collected was then manually examined using peak reflection analysis on a mineral presence/absence basis using the software DIFFRAC.SUITE. The data collected was then presented in an excel spreadsheet showing the presence or absence of certain minerals.
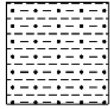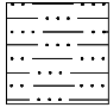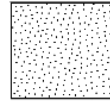
Six samples were chosen to undergo clay separation XRD to have a more in-depth understanding of the distribution of the clays present in these pits. These samples were selected upon their position within their pit, collecting one sample from the top part of the pit and one from the bottom. The samples selected were LTP001 55-60cm, LTP001 85-90cm, LTP002 50-55cm, LTP002 145-150cm, LTP003 45-50cm, LTP003 125-

130cm. Clay separation was carried out as per Tsao (2013) and XRD analysis was performed as outlined above.

Optically Stimulated Luminescence Dating

Nine samples were taken from the pits dug throughout the lunette sequence; four taken from LTP001, four taken from LTP002, one taken from LTP003 and one taken from Lake Torrens itself. These samples were dated using single-grain optically stimulated luminescence dating as per Aitken (1998), revealing the last time these sediments were exposed to light.

OBSERVATIONS

LTP001

Figure 3a A field photograph displaying the summary sample ranges (in red) and OSL locations (in black) for LTP001.
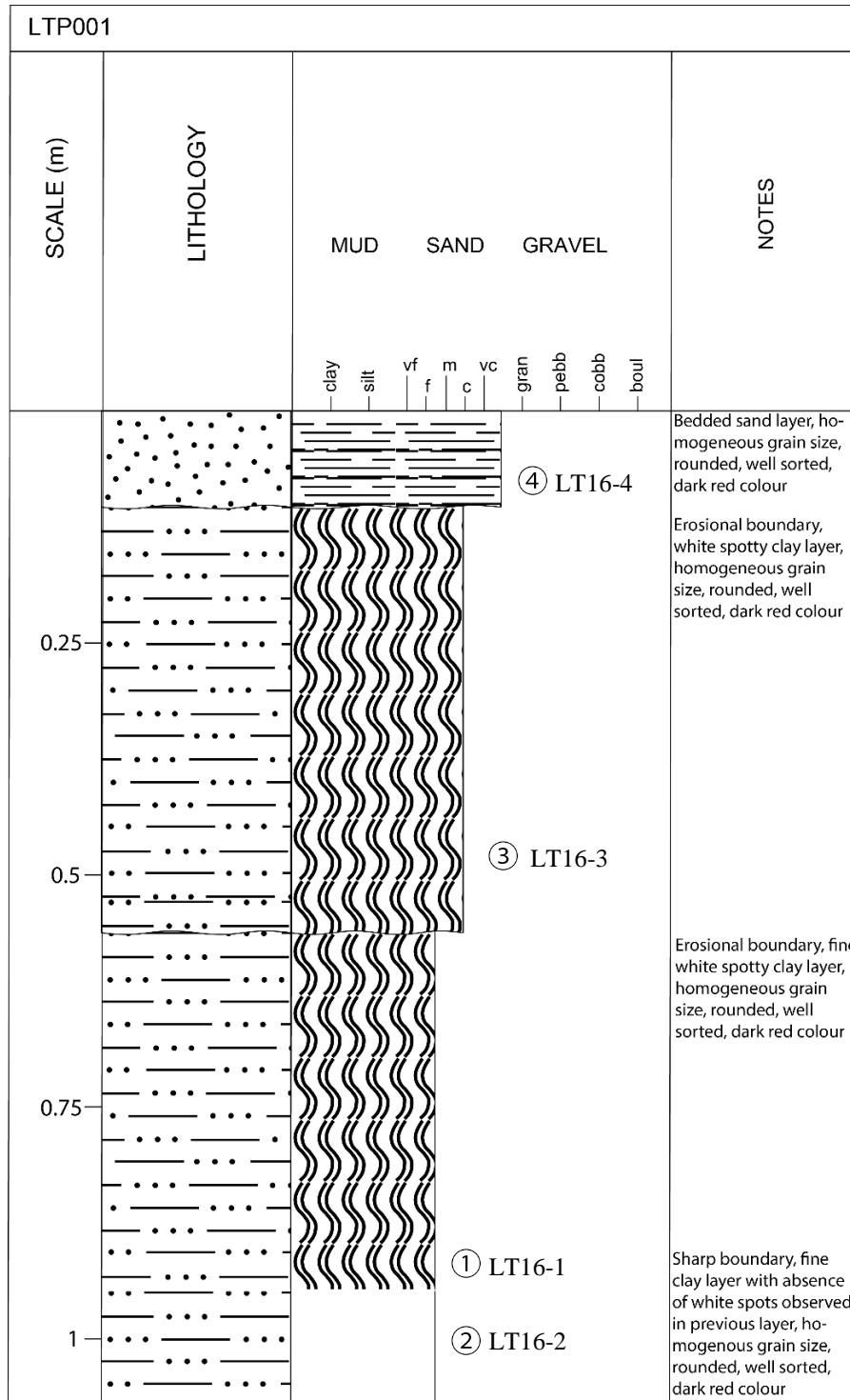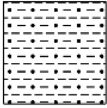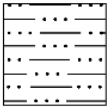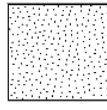
Figure 3b A stratigraphic log of Lake Torrens Pit 1 based on field observations showing four lithological units with characteristics of each unit.

LTP002

Figure 4a A field photograph displaying the summary sample ranges (in red) and OSL locations (in black) for LTP002.
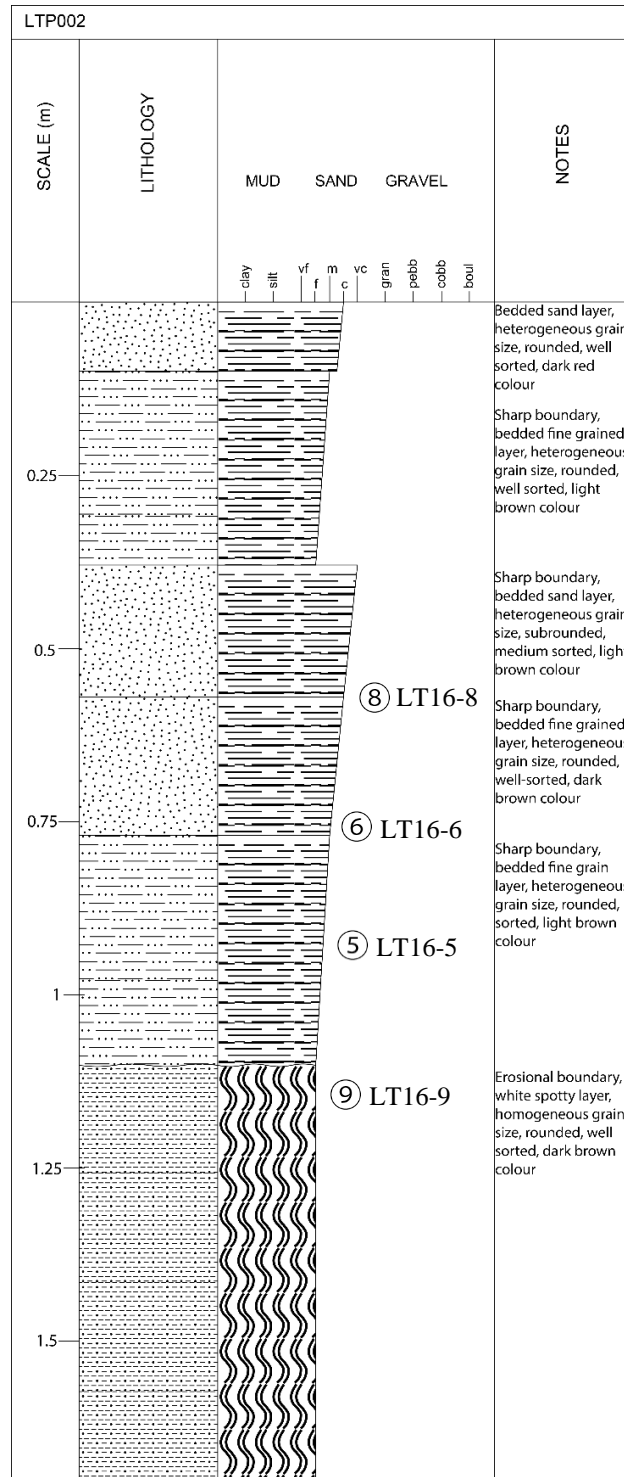
Figure 4b A stratigraphic log for Lake Torrens Pit 2 based on field observations showing six distinct lithological units consisting of sands, silts and clays.

LTP003
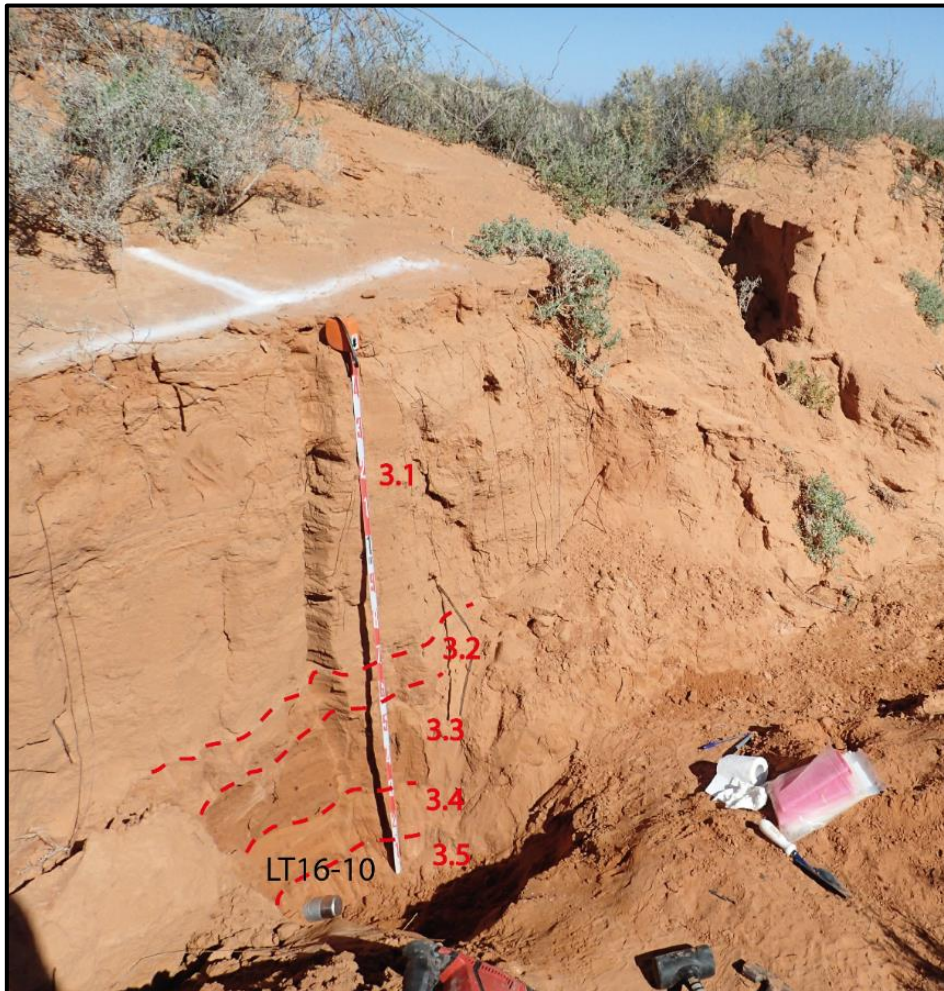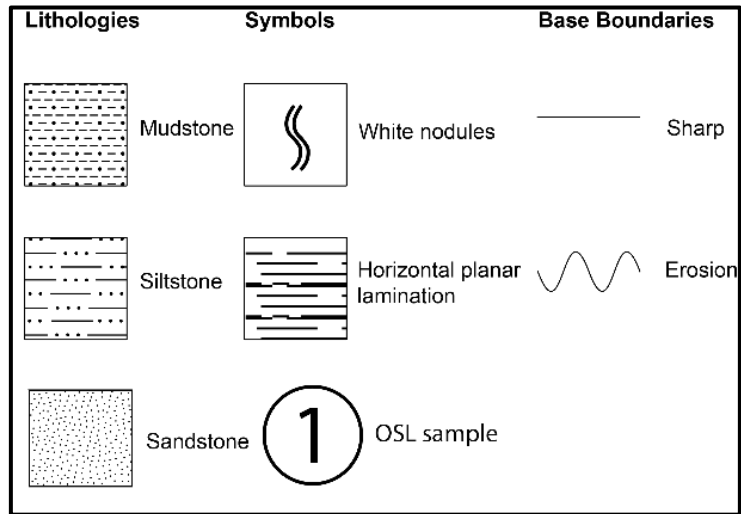
Figure 5a field photograph displaying the sample range locations (in red) and the OSL location (in black) for LTP003.
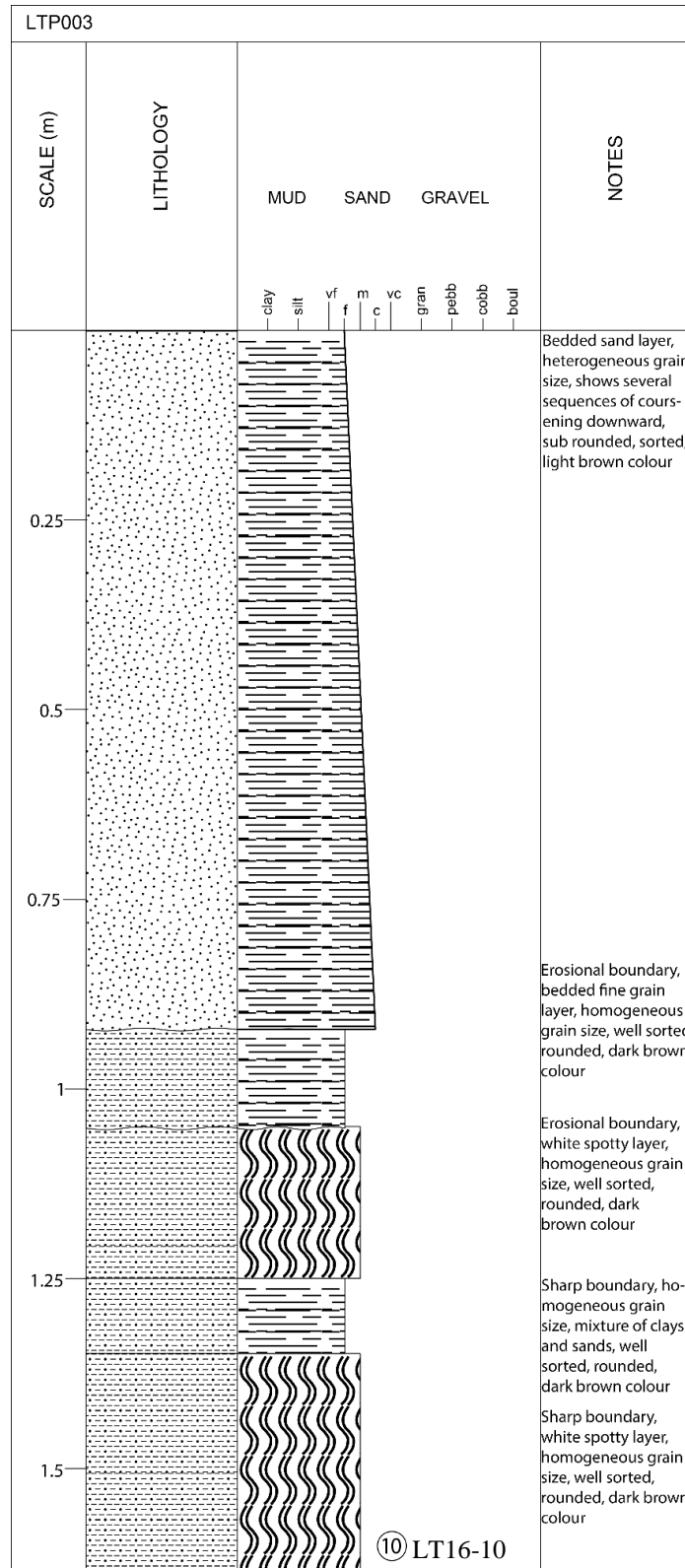
Figure 5b A stratigraphic log of Lake Torrens Pit 3 based on field observations showing five distinct lithological units consisting of sands, silts and clays

Lake Torrens

Figure 6 A field photograph displaying the OSL location for the pit dug in Lake Torrens.

RESULTS

Aerial Mapping via Drone Survey

The aerial mapping shows proximal distribution of units to each other and the offers an explanation for the results gathered throughout the study. Figure 7a immediately shows the scale of the study area and the distance of pits between each other. Features can immediately be observed in this figure which can be identified and characterised, as performed in figure 7b. This map shows more clearly the dispersion of units by giving them more obvious margins to other units. One of the most notable features from this map is the occurrence of clays, often forming in larger blowouts and narrow creek beds. A thick unit, labelled 'possible paleoshoreline' and characterised by vegetation, is found along the shoreline curving out into the Lake Torrens unit towards the bottom left section

of the map. This structure is then mimicked by a lighter colour unit (labelled 'gypsiferous unit'). Figure 7c and 7d describe the elevation throughout the study area, with Lake Torrens lower in elevation compared to the top of dune structure in the top right corner of the map. A significant observation that can be made if the elevation of these clay units showing that they sit lower than mobile sands and vegetation which surround them.
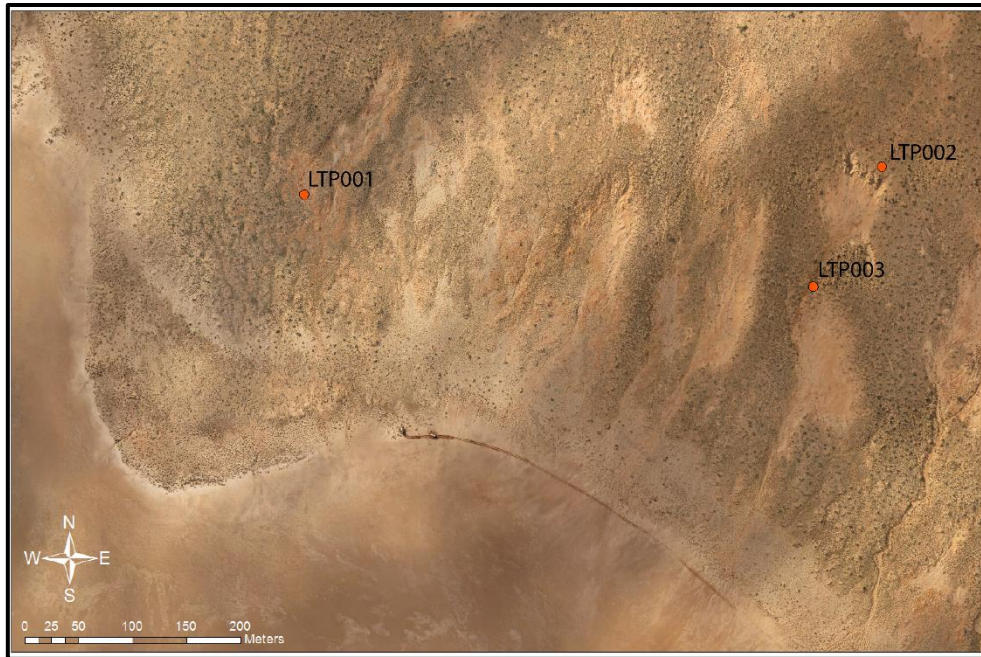
Figure 7a The original study area
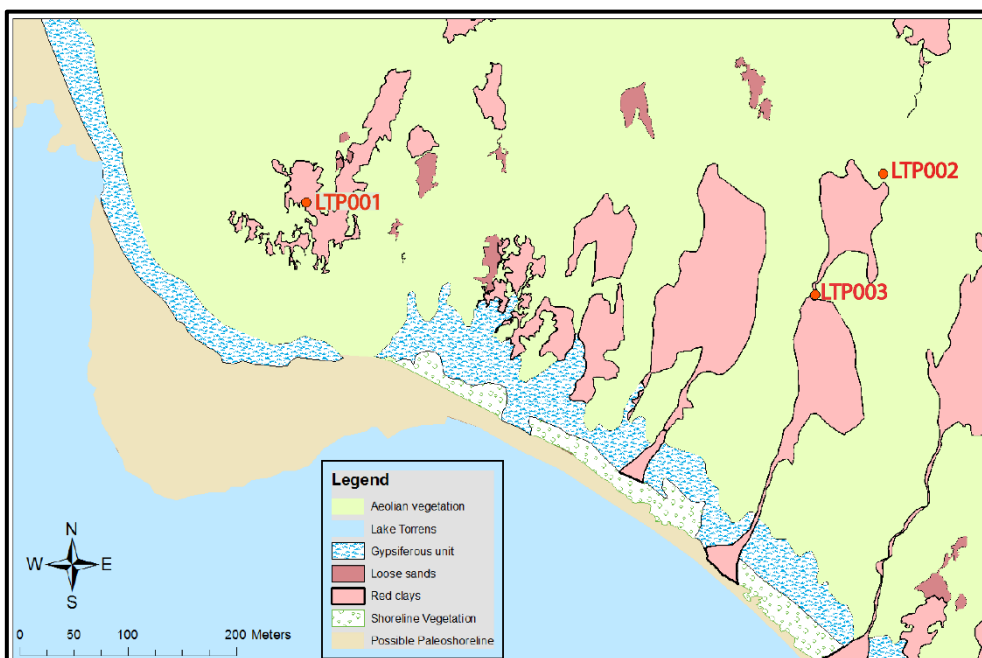
Figure 7b The study area after polygon characterisation showing the dispersal of units.
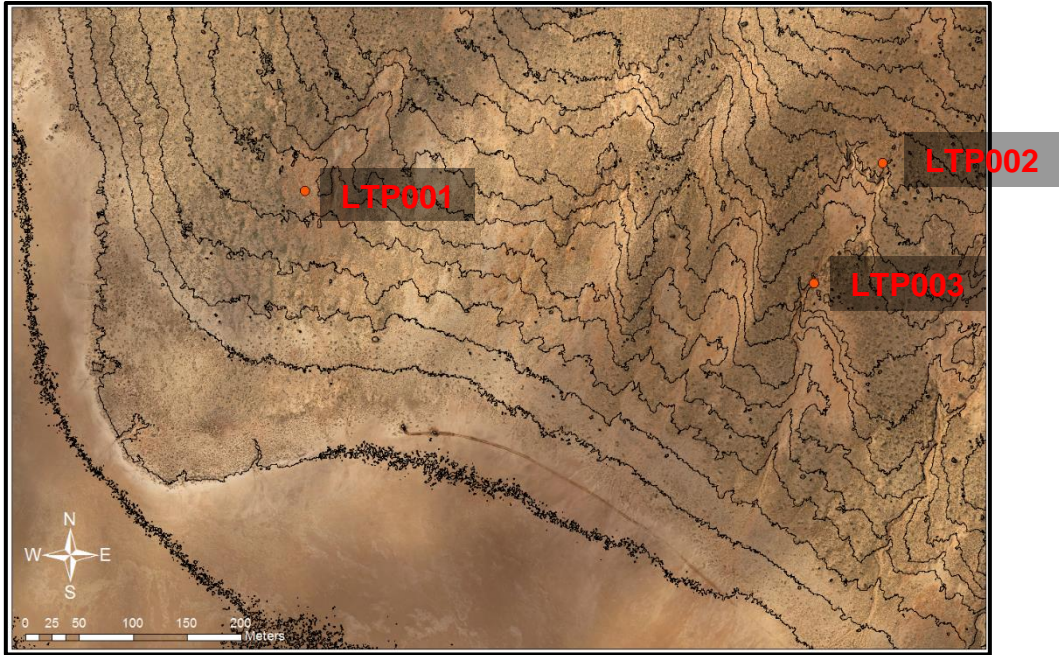
Figure 7c A contour map showing the elevation of the three pits dug relative to the Australian Height Datum throughout the study area.
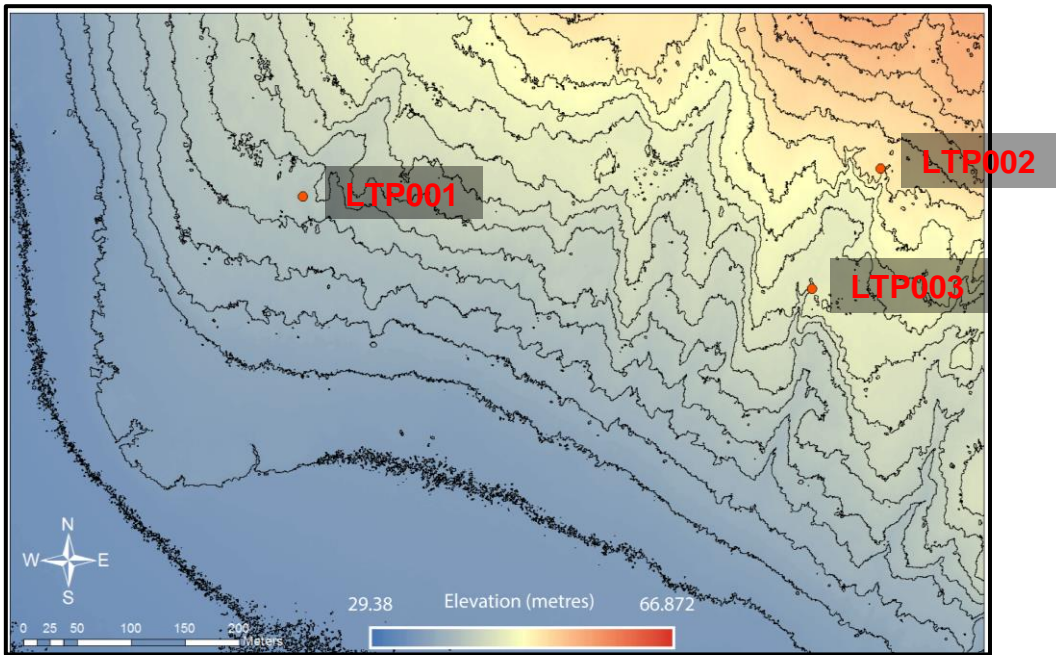
Figure 7d A digitally elevated modal with contour lines overlain showing the elevation of the study area with respect to sea level.

Stratigraphic logs

LTP001

This pit consisted of sands and sands mixed with clays broken up by erosional and sharp boundaries. The top unit consisted of horizontally bedded very course loose sands for 10 cm with an erosional lower boundary. The unit to follow from 10 cm to 55 cm consisted of a much tougher course grained sand mixed with silt which featured white rhizomorphs randomly throughout. The texture appeared to continue after an erosional boundary into the unit below until 93 cm in depth, however this layer appeared to have a lower abundances of white rhizomorphs. The fourth unit, from 93 cm to 110 cm, showed no rhizomorphs and consisted mainly of homogeneous silts however was tougher to dig through compared to the above layer.

LTP002

The top 5 cm consisted of horizontally bedded course sands which appeared to decrease in grain size with depth until reaching the unit below. Following a sharp transition was a horizontally bedded medium grained sand mixed with silt unit stretching to 38 centimetres in depth which decreased in grain size as it went down. Another sharp transition occurred at 38 cm which was proceeded by a horizontally bedded sand unit decreasing in size as it continued down to seventy 77 cm which offered a transition back to a sand mixed with silt unit. A white rhizomorph layer returned from 110 cm to 170 cm after a sharp transition from the previous unit.

LTP003

A large sand layer stretching for 93 cm which consist of several sequences of coarsening downward sequences. White rhizomorphs were observed close to the bottom of the pit with sequences of horizontally bedded muds mixed sand separating them.

Grain Size Analysis

The results from the Mastersizer 2000 offer percentage distributions of grain sizes for each sample analysed. Abundances of clay content never exceeded 4.46% throughout all the pits, with the ranges typically displaying more clay abundances occurring towards the bottom of all pits. However, results collected from the gravimetric analysis show much higher clay abundances for all samples (up to 18.28% in LTP001). Sand abundances tend to decrease with depth for all pits and gravel abundances tend to increase at the base of the pits.

LTP001 (table 2a & 2b) showed minimal clay abundance variation with depth in the Mastersizer results, remaining 1.11% to 2.05%. The gravimetric results, however, show much higher clay abundances throughout the pit, with higher percentages of clay occurring from 25-90 cm.

LTP002 (table 3a & 3b) showed minimal clay abundances similar to that of LTP001 in the Mastersizer results, only varying from 0.25% to 1.48%. There is a pattern observed though, with clay abundances increasing with depth. The gravimetric results support this pattern but offer higher clay abundance percentages.

LTP003 (table 4a & 4b) showed the most variation in clay percentage abundances in the Mastersizer results for all pits, varying from 0.78% at the top of the pit to 4.46% in the middle of the pit. The Mastersizer results suggest that clay abundances are highest in sample ranges 3.3-3.5, corresponding to depths 110-164cm (table 1.). This pattern is mimicked by the gravimetric results however, like the other two pits, show much higher clay percentages than the Mastersizer results.

A rise of clay abundances is also given in table 5 for the samples chosen to be investigated by clay separation XRD, displaying clay abundances up to 18.31%.

Tables 2a & 2b A summary of the grain size distribution of LTP001 using Mastersizer 2000 analysis (on the left) and gravimetric analysis distribution (on the right). The Mastersizer results show a substantial increase in finer grain sizes and decrease in larger grain sizes, with the exception of gravel, as depth continues. This correlates well with the values found through the Stokes' Law analysis, showing a higher abundance of clay sized particles can be observed from 25-90 centimetres.

Sample	Gravel (%)	Sand (%)	Silt (%)	Clay (%)
1.1	0.63	80.97	17.30	1.11
1.2	5.63	64.89	27.44	2.05
1.3	5.99	66.06	26.16	1.79
1.4	22.81	56.43	18.73	2.03

Sample	Sand + Silt Percentage (%)	Clay Percentage (%)
LTP001 5-10	91.12	8.88
LTP001 25-30	84.96	15.04
LTP001 55-60 (2)	81.72	18.28
LTP001 70-75	83.79	16.21
LTP001 85-90	82.35	17.65
LTP001 95-100	90.07	9.93

Table 3a & 3b A summary of grain size distribution of LTP002 using Mastersizer 2000 analysis (on the left) and gravimetric analysis distribution (on the right). The Mastersizer results show an extended sequence of courser grained material at the top of the pit which continues to finer grained clays and silts towards the bottom of the pit. This is consistent with results found using Stokes' Law analysis with the values down until 100 centimetres displaying a lower proportion of clay sized particles after which a small increase in clay abundance is shown.

Sample	Gravel (%)	Sand (%)	Silt (%)	Clay (%)
2.1	3.60	92.40	3.75	0.25
2.2	2.21	91.37	5.61	0.83
2.3	0.58	94.66	4.42	0.34
2.4	0.25	93.44	5.14	1.17
2.5	2.32	76.59	19.61	1.48
2.6	7.26	71.21	20.52	1.02

Sample	Sand + Silt Percentage (%)	Clay Percentage (%)
LTP002 0-5	95.55	4.45
LTP002 20-25	95.39	4.61
LTP002 50-55	95.29	4.71
LTP002 60-65	94.52	5.48
LTP002 90-95	91.09	8.91
LTP002 145-150	86.41	13.59
LTP002 165-170	90.96	9.04

Table 4a & 4b A summary of grain size distribution of LTP003 using Mastersizer 2000 analysis showing an large sand dominated samples range at the top of the pit transtioning to the bottom four sample ranges showing higher percentages of silt and clay content. This is supported by results found with gravimetric analysis distribution showing a large increase in clay percentage from 100 cm downwards.

Sample	Gravel (%)	Sand (%)	Silt (%)	Clay (%)
3.1	1.03	89.09	9.10	0.78
3.2	4.87	70.98	22.57	1.58
3.3	2.79	70.44	22.31	4.46
3.4	2.57	68.59	25.21	3.63
3.5	7.60	61.98	27.36	3.05

Sample	Sand + Silt Percentage (%)	Clay Percentage (%)
LTP003 45-50	93.99	6.01
LTP003 85-90	92.93	7.07
LTP003 100-105	90.99	9.01
LTP003 125-130	85.39	14.61
LTP003 135-140	91.00	9.00
LTP003 150-155	87.25	12.75

Table 5 Displays the Gravimetric analysis results clay abundances for the six samples chosen to have clay identification undertaken.

Sample	Sand + Silt Percentage (%)	Clay Percentage (%)
LTP001 55-60	81.69	18.31
LTP001 85-90	82.35	17.65
LTP002 50-55	95.29	4.71
LTP002 145-150	86.41	13.59
LTP003 45-50	93.99	6.01
LTP003 125-130	85.39	14.61

Optically Stimulated Luminescence

The dates collected in study (table 6) range from 0.17 ka (±0.07) until 382.39 ka (±87.22) with varying amounts of overdispersion and standard errors. LTP001 shows two dates very similar in LT16-1 and LT16-2 once the overdispersion and standard error of LT16-1 is considered. The youngest date from this pit is 1.62 ka from LT16-4 which shows and overdispersion of 13.751% suggesting that this age could be even younger. There are several younger dates which overlay LT16-9 in LTP002, with the youngest occurring in LT16-8. However, between 95 cm and 115 cm there is change in age of ~40 ka. LT16-10 was the only sample collected from LTP003 which showed a date similar to that found at the bottom of LTP001, and was sampled from a similar lithological unit. The only sample collected from Lake Torrens was LT16-7 which can only be used as a minimum age estimate because the natural signal exceeds the upper range of OSL dating. This sample showed huge overdispersion of the calculated dose equivalents and standard error for the calculated age.

Figure 8a A summary of calculated dose equivalent rates for LTP001.
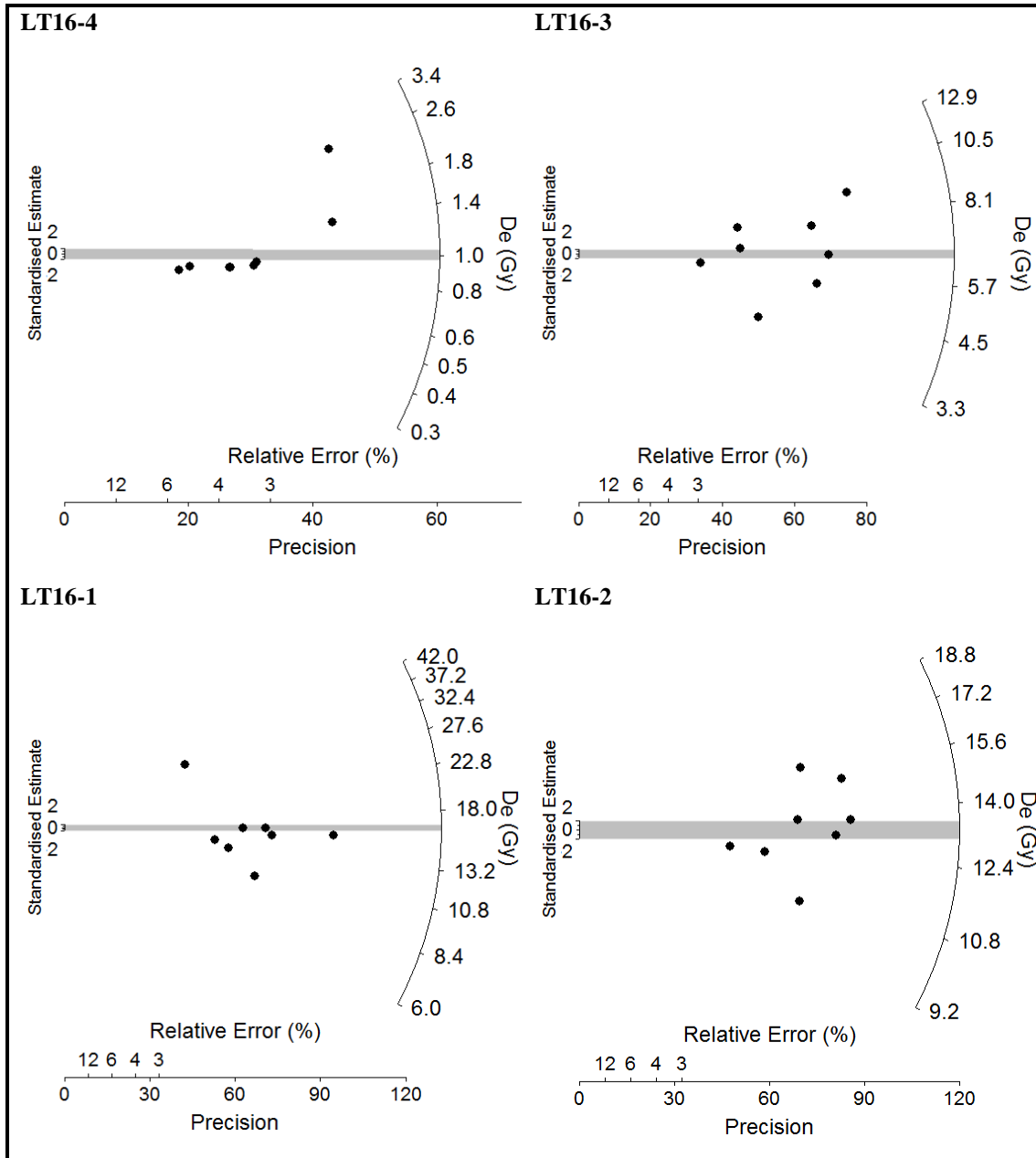
The dose equivalents calculated for LTP001 show little variability between grains. The samples which showed the greatest scatter was LT16-4, which sampled a sand rich unit at the top of the pit, and LT16-1, which was sampled at the bottom of the pit.

Figure 8b A summary of calculated dose equivalents rates for LTP002.
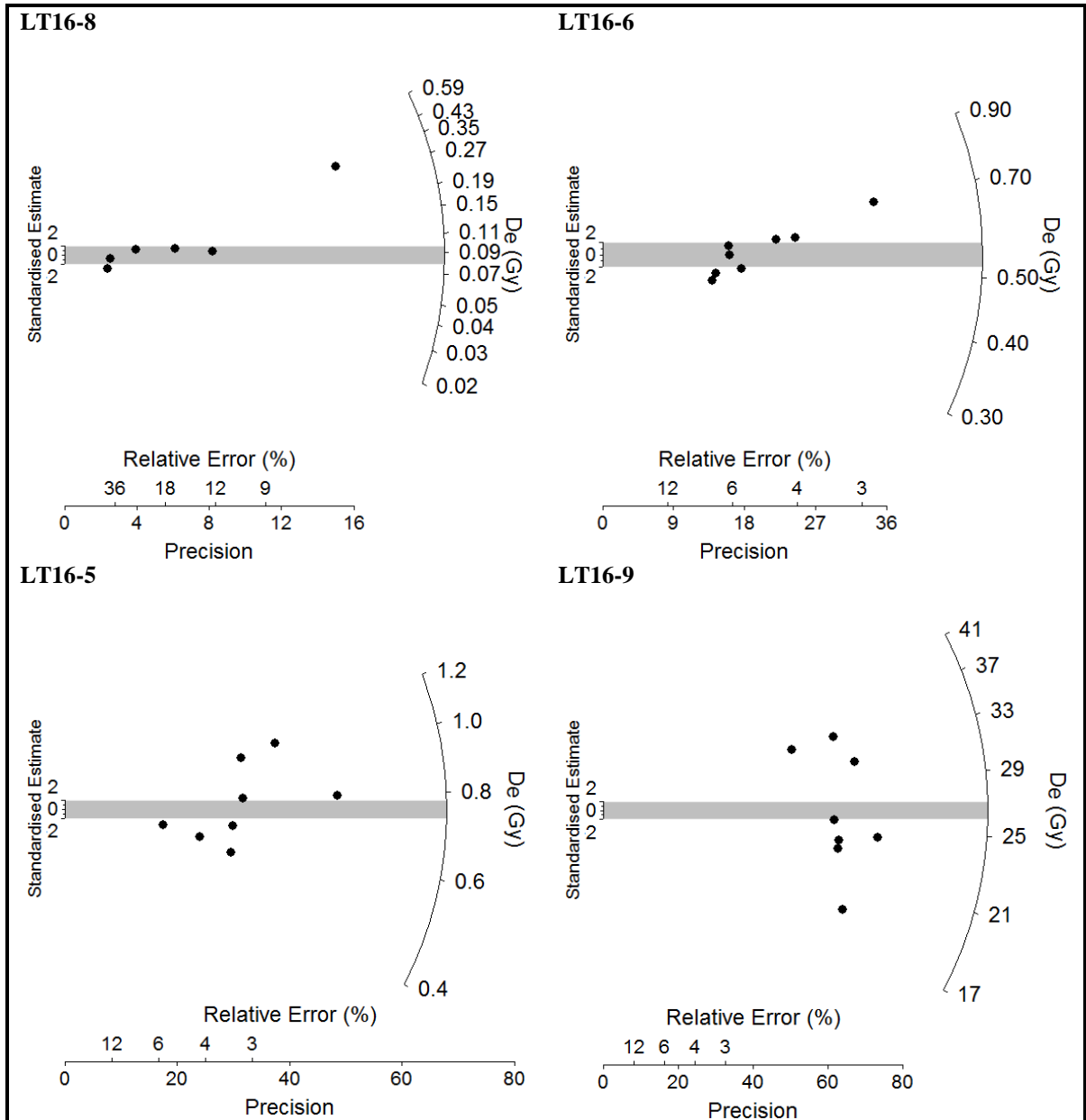
All dose equivalents calculated for LTP002 show minimal variability between grains besides LT16-9. This sample was collected from the bottom of the pit and shows considerable scatter, however shows minimal relative error and high precision for the dose equivalents calculated.

Figure 8c A summary of dose equivalent rates for LTP003.
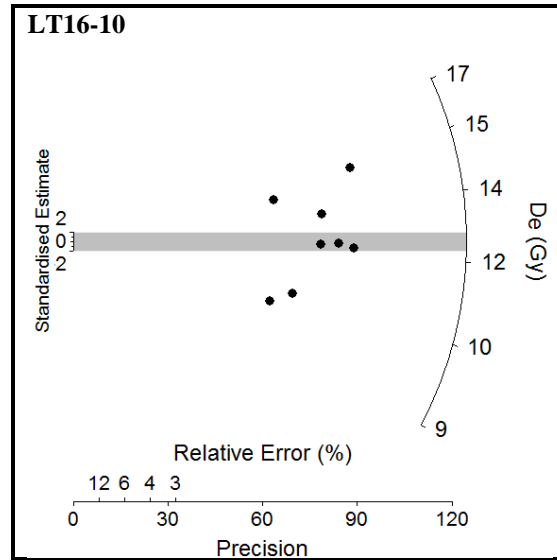
There was only one sample collected from LTP003 which showed minimal scatter in dose equivalent values for each grain. This sample shows minimal relative error and moderate precision in the collection of these dose equivalents.

Figure 8d A summary of dose equivalent rates for the pit dug in Lake Torrens.
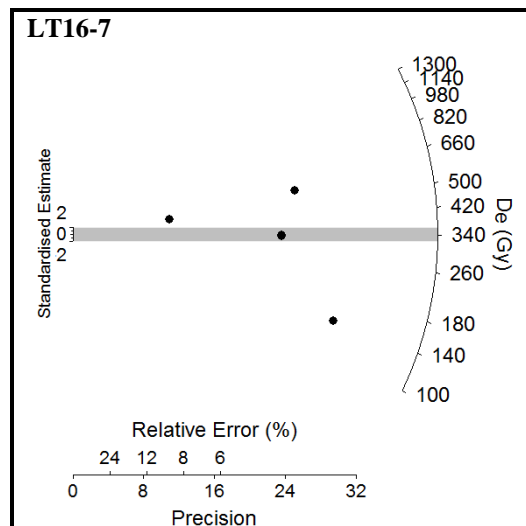
There was only one sample collected from LTP003 which showed a considerable amount of scatter of dose equivalents for the grains which could be calculated. Four of the grains could not reproduce a dose equivalent value and the grains that could showed high relative error and very low precision.

Table 6 A summary of all OSL dates collected while in the field.

Sample	Dose Rate (Gy)	Standard Error (Gy)	Dose Equivalent (Gy)	Standard Error (Gy)	Over-dispersion (%)	Location	Depth (cm)	Age (ka)	Standard Error (ka)
LT16-4	0.630	0.032	1.018	0.140	13.751	Pit 1	20	**1.62**	0.24
LT16-3	0.783	0.036	6.533	0.620	9.494	Pit 1	50	**8.34**	0.90
LT16-1	0.666	0.037	16.440	2.349	14.287	Pit 1	95	**22.16**	3.38
LT16-2	0.742	0.034	13.295	0.582	4.376	Pit 1	100	**19.95**	1.39
LT16-8	0.526	0.030	0.087	0.038	43.857	Pit 2	55	**0.17**	0.07
LT16-6	0.614	0.031	0.541	0.034	6.207	Pit 2	75	**0.88**	0.07
LT16-5	0.631	0.032	0.756	0.068	8.926	Pit 2	95	**0.40**	0.103
LT16-9	0.666	0.033	25.998	1.912	7.355	Pit 2	115	**39.04**	3.55
LT16-10	0.769	0.035	12.358	0.537	4.346	Pit 3	165	**16.08**	1.06
LT16-7	0.904	0.055	345.692	75.637	21.880	Lake Floor	45	**382.39**	87.22

X-Ray Diffraction

The results collected from X-ray diffraction of all samples showed a heterogeneous distribution of minerals throughout every pit. Quartz remains present throughout all depths with kaolinite also present for LTP001, LTP002 and most of LTP003. Other clays such as palygorskite had a variable presence, occurring frequently in LTP001 and LTP003 however showed infrequent appearances throughout LTP002, occurring more regularly between 57 cm and 150 cm. Muscovite tended to follow the infrequent abundance pattern of palygorskite, appearing throughout LTP001 and LTP003 but only occurring between 57 cm and 150 cm in LTP002. Calcite showed frequent presence in LTP001, however was absent in the top 25 cm. LTP002 and LTP003 showed calcite more frequently occurring in the top of their pits with LTP002 showing a second area of prolonged calcite

presence from 130 cm to 170 cm. Gypsum was only found frequently in LTP001, with a

depth interval of 25 cm to 105 cm all showing the presence of gypsum.

Table 7a A summary of x-ray diffraction results from LTP001. Quartz and kaolinite are consistent throughout the pit with palygorskite regularly appearing from 25 cm down until 95 cm in depth. Calcite and gypsum also regularly appear from 30 cm downwards.

Sample (Depth)	Quartz SiO2	Kaolinite Al2Si2O5(OH)4	Palygorskite (Mg,Al)2Si4O10(OH).4(H2O)	Muscovite KAl2(AlSi3O10)(F,OH)2	Calcite CaCO3	Gypsum CaSO4·2H2O
LTP001 0-5cm	✓	✓			✓	
LTP001 5-10cm	✓	✓	✓	✓		
LTP001 10-15cm	✓	✓				
LTP001 15-20cm	✓	✓	✓	✓	✓	
LTP001 20-25cm	✓	✓	✓	✓		
LTP001 25-30cm	✓	✓		✓	✓	✓
LTP001 30-35cm	✓	✓	✓	✓	✓	✓
LTP001 35-40cm	✓	✓	✓	✓	✓	✓
LTP001 40-45cm	✓	✓	✓	✓	✓	✓
LTP001 45-50cm	✓	✓	✓	✓	✓	✓
LTP001 50-55cm	✓	✓	✓	✓	✓	✓
LTP001 55-60cm	✓	✓	✓	✓	✓	✓
LTP001 60-65cm	✓	✓	✓	✓	✓	✓
LTP001 65-70cm	✓	✓	✓	✓	✓	✓
LTP001 70-75cm	✓	✓	✓	✓	✓	✓
LTP001 75-80cm	✓	✓	✓	✓	✓	✓
LTP001 80-85cm	✓	✓	✓	✓	✓	✓
LTP001 85-90cm	✓	✓	✓	✓	✓	✓
LTP001 90-93cm	✓	✓	✓	✓	✓	✓
LTP001 93-95cm	✓	✓	✓	✓	✓	✓
LTP001 95-100cm	✓	✓		✓	✓	✓
LTP001 100-105cm	✓	✓			✓	✓

Table 7b A summary of x-ray diffraction results from LTP002. Clay layers are found from 57 centimetres to 155 centimetres with varying presence of calcite and muscovite.

Sample (Depth)	Quartz SiO2	Kaolinite Al2Si2O5(OH)4	Palygorskite (Mg,Al)2Si4O10(OH).4(H2O)	Muscovite KAl2(AlSi3O10)(F,OH)2	Calcite CaCO3	Gypsum CaSO4·2H2O
LTP002 0-5cm	✓	✓				
LTP002 5-10cm	✓	✓			✓	
LTP002 10-15cm	✓	✓		✓	✓	
LTP002 15-20cm	✓	✓			✓	
LTP002 20-25cm	✓	✓	✓	✓		
LTP002 25-30cm	✓	✓			✓	
LTP002 30-35cm	✓	✓				
LTP002 35-38cm	✓	✓			✓	
LTP002 38-40cm	✓	✓			✓	
LTP002 40-45cm	✓	✓	✓	✓	✓	
LTP002 45-50cm	✓	✓			✓	
LTP002 50-55cm	✓	✓			✓	
LTP002 55-57cm	✓	✓			✓	
LTP002 57-60cm	✓	✓	✓		✓	
LTP002 60-65cm	✓	✓	✓			
LTP002 65-70cm	✓	✓				
LTP002 70-75cm	✓	✓	✓	✓		
LTP002 75-77cm	✓	✓	✓	✓		
LTP002 77-80cm	✓	✓	✓			
LTP002 80-85cm	✓	✓	✓	✓		
LTP002 85-90cm	✓	✓	✓	✓		
LTP002 90-95cm	✓	✓		✓		
LTP002 95-100cm	✓	✓	✓	✓		
LTP002 100-105cm	✓	✓	✓	✓		
LTP002 105-110cm	✓	✓	✓	✓		
LTP002 110-115cm	✓	✓	✓	✓		
LTP002 115-120cm	✓	✓	✓	✓		
LTP002 120-125cm	✓	✓		✓		
LTP002 125-130cm	✓	✓	✓	✓		
LTP002 130-135cm	✓	✓		✓	✓	
LTP002 135-140cm	✓	✓	✓	✓	✓	
LTP002 140-145cm	✓	✓		✓	✓	
LTP002 145-150cm	✓	✓	✓	✓	✓	
LTP002 150-155cm	✓	✓				
LTP002 155-160cm	✓	✓		✓	✓	
LTP002 160-165cm	✓	✓		✓	✓	
LTP002 165-170cm	✓	✓		✓	✓	

Table 7c A summary of x-ray diffraction results from LTP003. A much more clay rich pit compared to the previous pits with varying abundances of calcite and gypsum.

Sample (Depth)	Quartz SiO2	Kaolinite Al2Si2O5(OH)4	Palygorskite (Mg,Al)2Si4O10(OH).4(H2O)	Muscovite KAl2(AlSi3O10)(F,OH)2	Calcite CaCO3	Gypsum CaSO4·2H2O
LTP003 0-5cm	✓	✓	✓	✓	✓	
LTP003 5-10cm	✓	✓	✓	✓	✓	
LTP003 10-15cm	✓	✓		✓	✓	
LTP003 15-20cm	✓	✓	✓	✓	✓	
LTP003 20-25cm	✓	✓	✓	✓	✓	
LTP003 25-30cm	✓	✓		✓	✓	
LTP003 30-35cm	✓	✓	✓	✓	✓	
LTP003 35-40cm	✓	✓	✓	✓		
LTP003 40-45cm	✓	✓	✓	✓		
LTP003 45-50cm	✓	✓	✓	✓		
LTP003 50-55cm	✓	✓	✓	✓		
LTP003 55-60cm	✓	✓	✓	✓		✓
LTP003 60-65cm	✓	✓	✓	✓	✓	✓
LTP003 65-70cm	✓	✓	✓	✓		
LTP003 70-75cm	✓	✓	✓	✓		
LTP003 75-80cm	✓	✓	✓	✓		
LTP003 80-85cm	✓	✓	✓	✓		
LTP003 85-90cm	✓	✓	✓	✓		
LTP003 90-92cm	✓	✓				
LTP003 92-95cm	✓		✓	✓		
LTP003 95-100cm	✓		✓			
LTP003 100-105cm	✓	✓	✓	✓		
LTP003 105-110cm	✓			✓		
LTP003 110-115cm	✓	✓	✓		✓	
LTP003 115-120cm	✓	✓	✓	✓		
LTP003 120-125cm	✓	✓	✓	✓		
LTP003 125-130cm	✓	✓	✓	✓		
LTP003 130-135cm	✓	✓	✓	✓		
LTP003 135-140cm	✓	✓	✓	✓		
LTP003 140-145cm	✓	✓	✓	✓	✓	
LTP003 145-150cm	✓	✓	✓	✓	✓	
LTP003 150-155cm	✓	✓	✓	✓	✓	
LTP003 155-160cm	✓	✓	✓	✓	✓	
LTP003 160-164cm	✓	✓	✓	✓	✓	

Clay Separation X-Ray Diffraction

Table 8 A summary of the results collected from clay separation x-ray diffraction that these samples contained chlorite, mica, palygorskite and kaolinite however uncertain presences regarding smectite, vermiculite and sepiolite.

Sample	Chlorite/ Smectite	Vermiculite/Chlorite	Mica	Palygorskite	Kaolinite	Sepiolite
LTP001 55-60 cm	✓	✓	✓	✓	✓	
LTP001 85-90 cm	✓	✓	✓	✓	✓	
LTP002 50-55 cm	✓	✓	✓	✓	✓	
LTP002 145-150 cm	✓	✓	✓	✓	✓	
LTP003 45-50 cm	✓	✓	✓	✓	✓	✓
LTP003 125-130 cm	✓	✓	✓	✓	✓	✓

X-Ray Fluorescence

The results shown from the x-ray fluorescence analysis (figures 9a-9d) of each samples shows that these pits have a variable elemental composition in relation to depth. Once the data collected was displayed as line graphs it is more obvious to see the interactions and correlations the elements have with each other. Elements were chosen to be displayed in a ratio with zirconium as this is an immobile element in the soil profile and useful for a true gauge on content (Stiles, Mora, & Driese, 2003). A noticeable relationship is the correlation between aluminium content and grain size. As grain size decreases, the silica content decreases and the aluminium content increases, summarised in the Al/Si line graph. LTP001 shows this relationship from 20 cm downwards, LTP002 shows this relationship from 35 cm downwards and LTP003 shows this relationship from 90 cm downwards. The calcium content in these pits can also be a useful indicator of carbonate content in the soil. The increase of calcium also shows a weak correlation in all pits with the decrease in grain size and increase in aluminium content. Once put in a ratio, calcium and sulphur are able to provide a reliable indicator of gypsum content when the ratio is equal to 1 ppm. This is observed in LTP001 from 90-100cm.
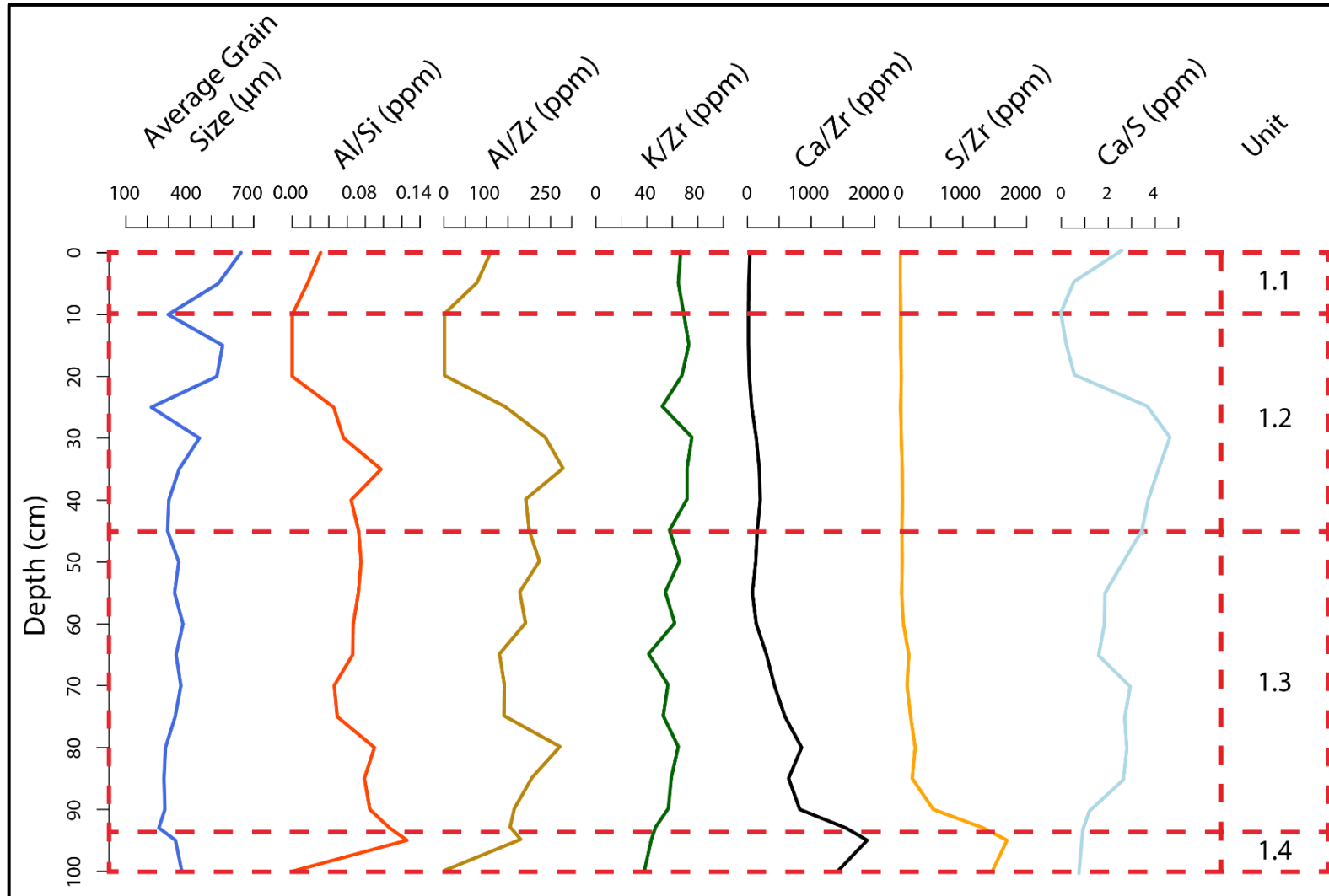
Figure 9a Line graphs comparing the output data collected from x-ray fluorescence with the average grain size collected from the Mastersizer 2000 for LTP001.
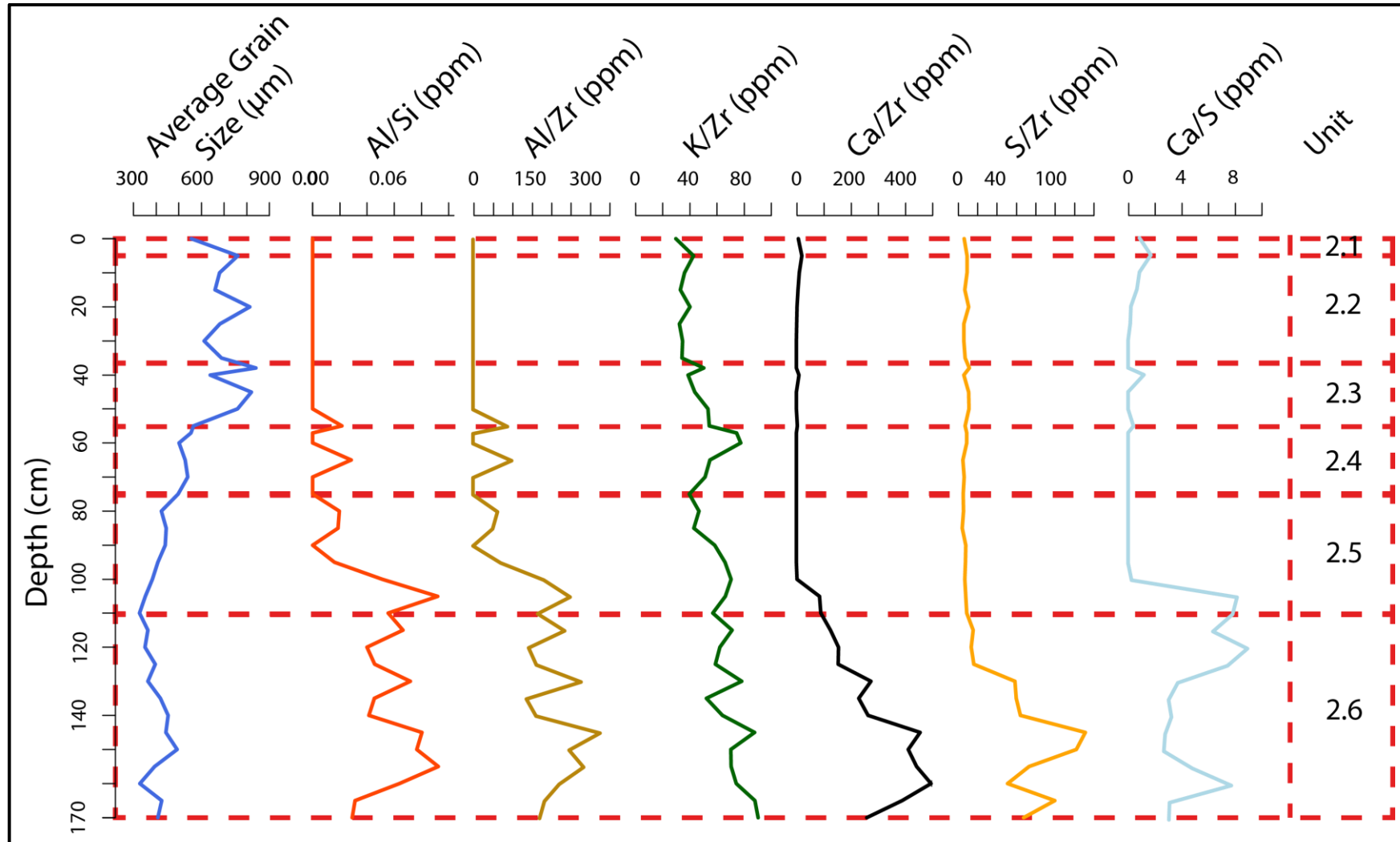
Figure 9b Line graphs comparing the output data collected from x-ray fluorescence with the average grain size collected from the Mastersizer 2000 for LTP002.
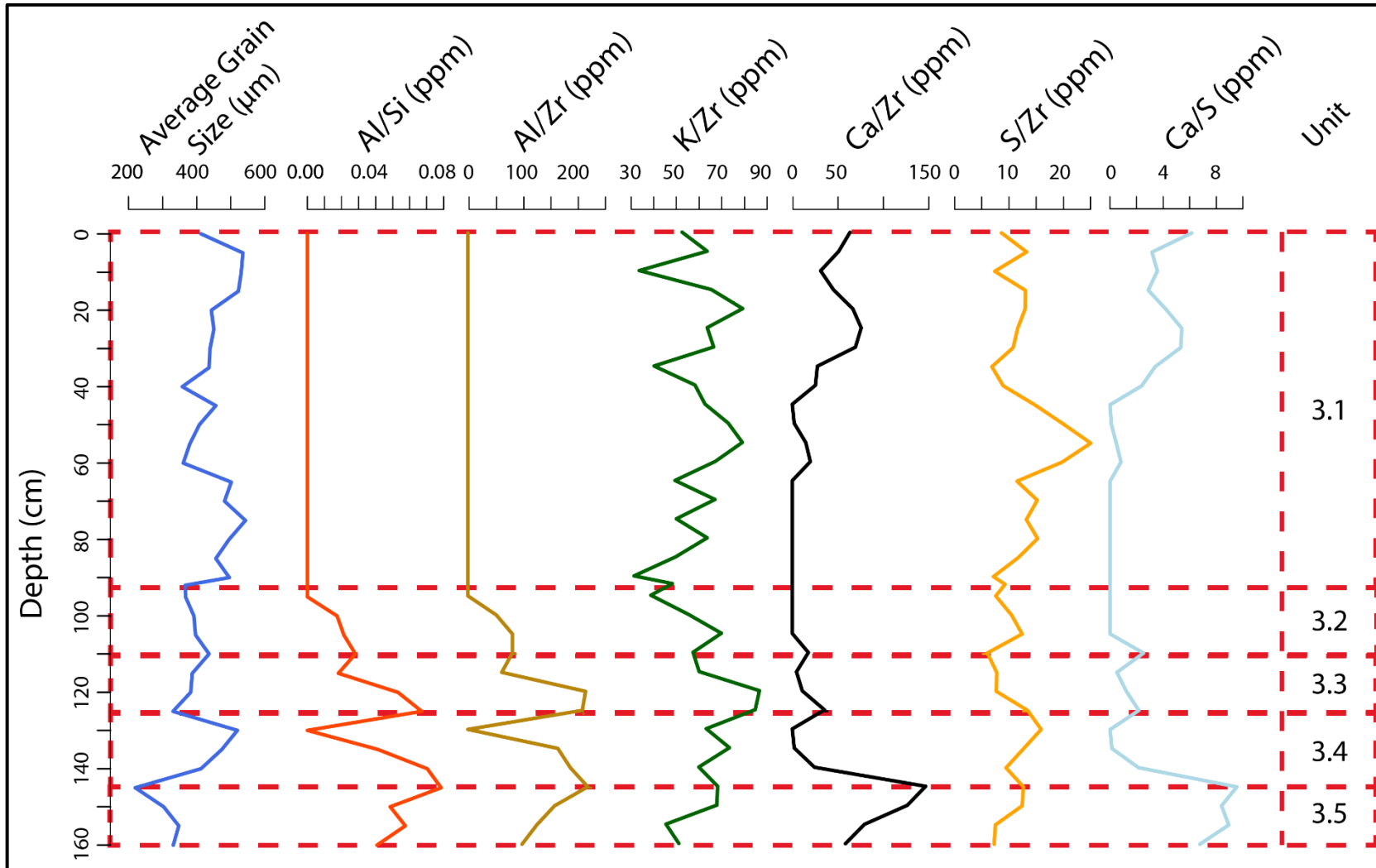
Figure 9c Line graphs comparing the output data collected from x-ray fluorescence with the average grain size collected from the Mastersizer 2000 for LTP003.

DISCUSSION

Based on the observations made in the field and results collected through a variety of methods it can be concluded that there are several lithological changes throughout the Lake Torrens shoreline study area. Aerial photogrammetry has shown the distribution of these units in the study area and also shown how these units relate to each other with elevation. There is a variety of grain size, elemental and mineralogical distinctions in respect to depth for each pit dug as outlined previously, all of which provides vital information in the reconstruction of paeloclimatic settings.

Analysis of lithologies

Through field observations and grain size analysis it is obvious that there are at least three different units making up the shoreline feature being investigated in this area. These units include the sand dune unit, clay unit and paleosol unit, all forming at different times and characterised by different elemental, mineralogical and grain size features.

The sand dune unit is a mobile unit found throughout the aerial photographs in the loose Aeolian vegetation and often surrounding the clay blowout units. This unit contains a relatively low clay content, represented in the lack of clays present in the top depths of XRD data and the low aluminium content shown in the XRF data. The ages on this unit suggests that this unit is quite young, ranging from 0.17 ka (±0.07) to 1.62 ka (±0.24), meaning it is not related to any lake filling/drying event. The clay content which can be observed in this unit can best be interpreted as originating from other sources other than the lake itself, perhaps blown in from clay blowouts which these sands surround or through fluvial activity bringing clays into the environment.

The lunette unit can be seen throughout the aerial photographs as clay blowouts and is immobile compared to the sand dune unit. This unit is much finer grained and contains

higher aluminium content, lower silica content, which is supported by the presence of clays palygorskite and kaolinite. The dates of the deposition show that these units have been immobile for up to 40 ka, with low amounts of erosion. This study concludes that these clays are associated with a lake drying event and there are two observed units from this lithology.

The paleosol unit can be seen beneath clay units through the pits dug. This unit has a small grain size similar to the lunette unit however differ elementally and mineralogically. An increase of calcium can be observed in these layers, which is supported by the XRD data showing presence of calcite. This is supported by observations of 'white rhizomorphs' within a clay rich unit. These white rhizomorphs are interpreted as being remnants of rhizoliths migrating through the soil indicating that a period of humidity had occurred. However, the dates from this unit can be misleading as they depict the date the sediments were deposited, with soil formation and vegetation cultivation forming as a post depositional event. These dates can still retain some significance in providing these units with a minimum age of deposition.

This leads to three time dependent events occurring throughout the study area; deposition of sediments, soil formation/vegetation cultivation and erosion of features. The OSL dating completed in this study is limited in exclusively offering the time of deposition of these samples, and the other two events must be inferred upon.

Analysis of data

From the data collected and making the assumption made by Bowler (1973) that a high clay content lunette is indicative of a drying lake period it is then possible to assign each unit to a wet or dry phase of the lake's history.

The results shown in the aerial photos offer an insight into the relative timing of events utilizing fundamental laws of dating. Elevation modelling uses the law of Superposition showing clay units below sands and vegetation, which can indicate that the clay units found throughout the area were deposited earlier and are older than the loose sands and aeolian vegetation. Cross cutting relationships can also be observed within this map, showing clays creating an alluvial fan structure cutting through shoreline vegetation and gypsiferous units. These cross cutting relationships can be related to post depositional fluvial activity, suggesting that fluvial activity increased after the formation of the shoreline vegetation and gypsiferous units and transported clays towards the shoreline. The relative ages for each unit shown in the aerial photography are (from youngest to oldest);

- Aeolian vegetation

- Shoreline vegetation

- Possible paleoshoreline

- Gypsiferous unit

- Loose sands

- Red clays

- Lake Torrens

Not only can these observations provide a rough guide to the ages of these units, they can also offer information about the textural characteristics through their response to erosion. It can be observed that the loose sands and aeolian vegetation can be quickly eroded to expose a lower lying clay unit, suggesting that these clays are more resilient than sands after deposition.

The grain distribution results provided by the Mastersizer 2000 has been proven to be the useful indicator of comparative course grain vs. fine grain layers however limited with absolute values of grain sizes due to instrument error. In this study we did not use a clay dispersant and the results showed lower than expected clay percentages, suggesting clay aggregation had occurred while suspended in deionized water. High clay concentrations can lead to electrostatic face-to-face, edge-to-edge and edge-to-face attraction which can result in aggregation of clays. Dispersants such as sodium hexametaphosphate, sodium polyacrylate and sodium polyphosphate are all capable clay dispersants which, when applied, can modify the particle surface to enhance the electrostatic repulsion between clays (Ming et al., 2016). However when compared to the results found in the Gravimetric distribution analysis the distribution of clay sizes remained consistent, with variations in the absolute abundances of grain sizes.

The sample ranges which showed considerably higher clay content through Gravimetric distribution analysis consisted of;

- 1.2 & 1.3

- 2.5 & 2.6

- 3.3, 3.4 & 3.5

The percentages of clay content for each of these sample ranges varies from 9-18% which are similar results Bowler (1973) found from South Australian lunette examples at Hutton's Lagoon, Hynam Swamp, Cockatoo Lake and Lochaber Swamp. These inferences are supported by these sample ranges showing high aluminium content in the XRF data and also showing presence of clays throughout the XRD data.

The origin of these clay rich units found surrounding Lake Torrens are assumed to be associated with a lake drying event, however the size of these clay units and their

mineralogical composition offer information about the settings at the time of their deposition. Lunettes typically take thousands of years to form, accumulating clays from the nearby lake drying out, which would correspond to a large clay unit observed in the sedimentary log. The mineralogical composition of these clay units has been outlined in XRD analysis, firstly during bulk analysis and secondly after the clays were separated. Authigenic clays can have a unique ability to offer information regarding the settings of paleoclimates at the time of deposition and controls leading to the genesis of clays. Many authigenic clays found in salt lakes and playa lakes are detrital and reflect the composition of argillaceous formations in the palaeodrainage areas (Fisher, 1988). The pits dug throughout the Lake Torrens shoreline show a high frequency of kaolinite and chlorite and also the presence of palygorskite in the finer grained areas. The dispersal of palygorskite, in particular, is of significance as natural occurrences of palygorskite have been reported in sediments from soils of arid regions, as well as wet lacustrine settings (Long et al., 1997). A possible explanation for the formation of the palygorskite is the fall in water table during the onset of a dry phase, exposing low-lying areas to soil forming processes; converting smectite-rich soils and sediments into palygorskite.

Timing of wet and dry periods at Lake Torrens

The sedimentary evidence from Lake Torrens is interpreted to reflect distinct periods of wet and dry climate. The presence of aeolian sediments on a regional scale deposited from suspension provides convincing proof of arid environments. The data collected in through x-ray diffraction and x-ray fluorescence further supported the interpretation of these clay-rich dry phase layers. However, the explanation of the timing of these events is still more complicated. The dates collected show dry periods occurring in this area from ~8.34 kyr until ~20kyr in LTP001, at ~39.04 kyr in LTP002 and ~16.08 kyr in LTP003 (table 13).

This leads to several interpretations as to the distribution of these phases and the correlation these have with structures throughout the area.

Table 9 The ages of all OSL samples collected with orange samples represents a dry arid phase and blue samples representing a younger loose sands.

Sample	Dose Rate (Gy)	Standard Error (Gy)	Dose Equivalent (Gy)	Standard Error (Gy)	Over-dispersion (%)	Location	Depth (cm)	Age (ka)	Standard Error (ka)
LT16-4	0.630	0.032	1.018	0.140	13.751	Pit 1	20	**1.62**	0.24
LT16-3	0.783	0.036	6.533	0.620	9.494	Pit 1	50	**8.34**	0.90
LT16-1	0.666	0.037	16.440	2.349	14.287	Pit 1	95	**22.16**	3.38
LT16-2	0.742	0.034	13.295	0.582	4.376	Pit 1	100	**19.95**	1.39
LT16-8	0.526	0.030	0.087	0.038	43.857	Pit 2	55	**0.17**	0.07
LT16-6	0.614	0.031	0.541	0.034	6.207	Pit 2	75	**0.88**	0.07
LT16-5	0.631	0.032	0.756	0.068	8.926	Pit 2	95	**0.40**	0.103
LT16-9	0.666	0.033	25.998	1.912	7.355	Pit 2	115	**39.04**	3.55
LT16-10	0.769	0.035	12.358	0.537	4.346	Pit 3	165	**16.08**	1.06
LT16-7	0.904	0.055	345.692	75.637	21.880	Lake Floor	45	**382.39**	87.22

As shown from the aerial photos collected in figures 5-7 the distribution of these pits throughout the lunette sequence varies in longitude, latitude and elevation, which could all affect the distribution of these phases. LTP001 and LTP003 are found at a similar elevation as shown in the figure 7 elevation map, and also show a clay-rich paleosol of approximately the same age with sand mixed with clay layer capping it. This could be assumed to be the same unit expressed in different areas of the map. LTP002 shows a much older paleosol at the base of the pit with very young sands mixed with clays above it. This paleosol was not seen at the two other pits closer to the shoreline, most probably due to their elevation compared to LTP002, which leads to the suggestion that an

erosional event occurred which cleared away remaining paleosol from LTP002, creating accommodation space for younger sands and clays to be deposited, summed up in figure 11.

This study concludes that two drying events are recorded in this lunette structure, one occurring at ~40 ka and another occurring at ~20 ka (figure 10). A primary assumption in this hypothesis, however, is that the clay rich unit found at the base of LTP003 and LTP001 are from the same drying event, with LTP002 recording a separate event. We can suggest that a humid phase must have occurred between 40 ka and 20 ka and then again between 20 ka and 8 ka for the formation of the paleosol units observed at the base of the three pits. This is supported by lake levels found from Lake Frome suggesting a higher lake level at these times, indicating a wet phase occurring in the region. This would suggest a low clay abundance unit would be observed below the paleosol units found in LTP001 and LTP003. Furthermore it can be suggested that a wet phase could be observed before ~40 ka, to provide enough moisture for clays to dry out and form clay rich lunette units.
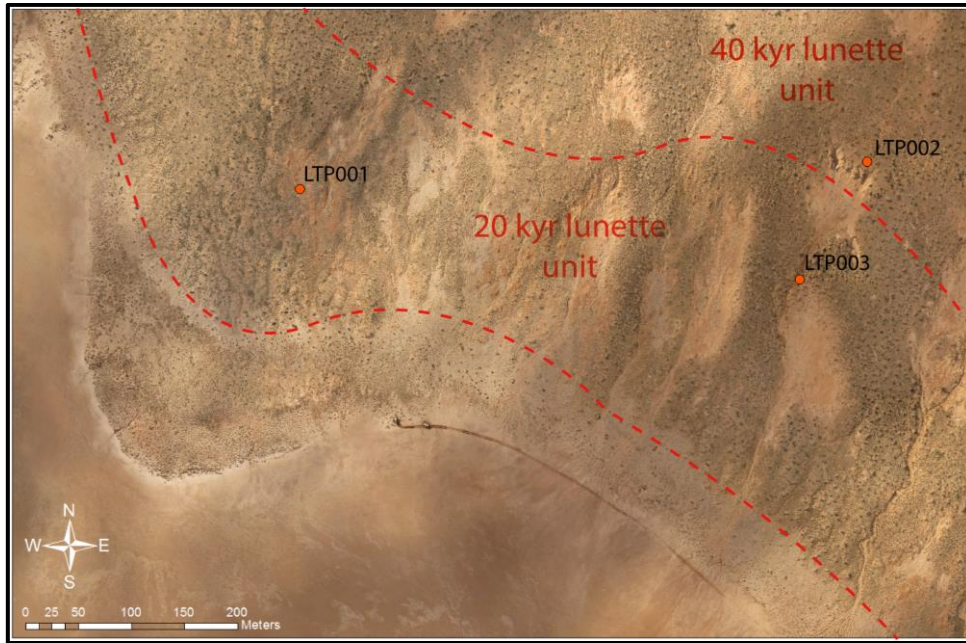
Figure 10 The original study area with overlain interpretations of dates for the two lunette forming ages events.

The hypothesis of a constant drying and accumulation of clays from ~40ka until at least ~8ka is possible because we have no dates between ~40 ka and ~20 ka to constrain an event however it is uncharacteristic for lunettes and dry periods in Australia to occur over a period of 20 ka (Fitzsimmons et al., 2013) and is therefore unlikely to be the case for Lake Torrens. Evidence to support the invalidity of this hypothesis lies within the data collected in the XRF results. This hypothesis suggests that the lunette sequence found in samples range 3.5 is the top of sample range 2.6, with the overlying sediments being eroded away in LTP002. The XRF results for sample range 3.5 shows considerably lower abundances of aluminium and calcium when compared to 2.6 which suggests these units are not related.
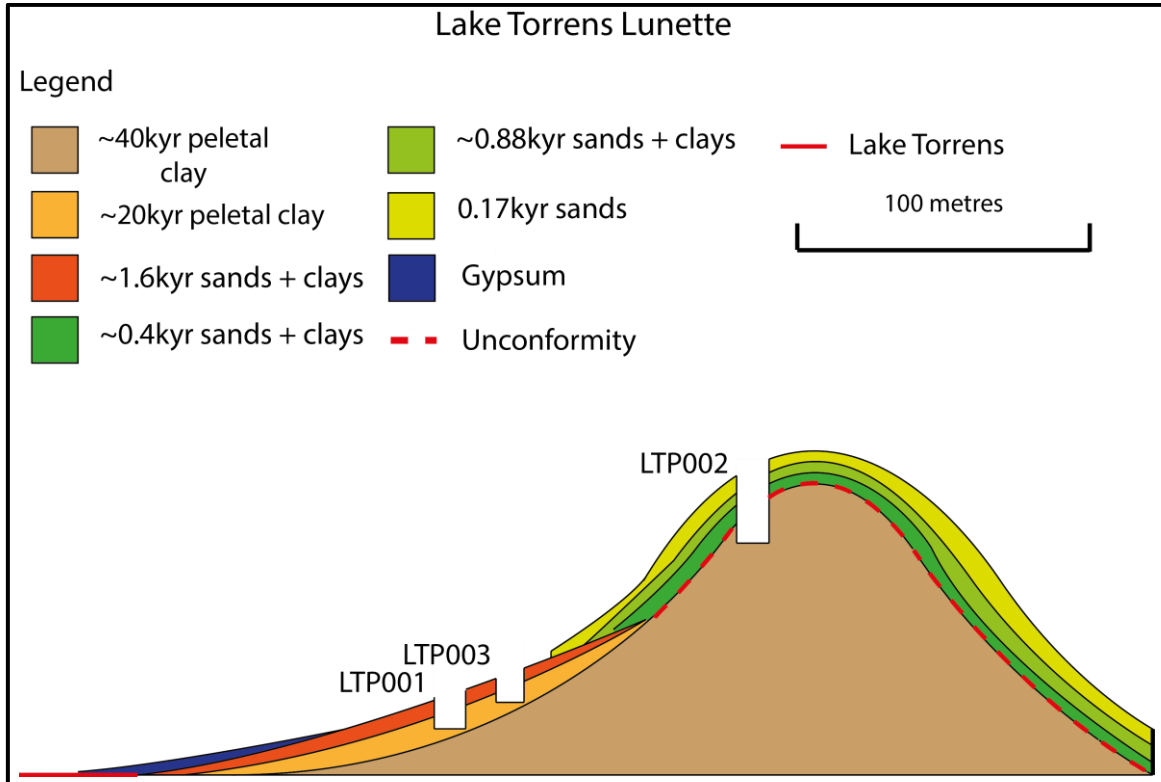
Figure 11 Displays a simplified cross section of the lunette sequence studied. Most notable is the unconformity which observed by LTP002 with approximately 40ka years of record missing. Change labels eg 40kyr peletal clay, sands + clays indicate interbedded sands and clays

Lake Torrens vs surrounding lakes.

In an attempt to compare inland lakes against other inland lakes Bowler (1981) created an equation leading towards a hydrologic classification based on combinations of catchment and climatic-hydrologic characteristics. As defined by Bowler, the controlling factors for any terminal lake system can be defined as:

$$Water\ in = Al{\times}P + (Ac - Al)Pf$$

Where:

$$Ac = Area\ of\ catchment$$

$$Al = Area\ of\ lake\ water\ surface$$

$$P = Mean\ annual\ precipitation$$

$$E = Mean\ annual\ evaporation$$

$$Pf = runoff{\times}P$$

44

Under conditions experienced today for inland the runoff coefficient usually never exceeds 10%. However, cases have been observed in up to 30% after brief high-intensity rainstorms. Therefore this equation accounts for a range of runoffs coefficient values, from $0.1{\times}P$ to $0.3{\times}P$. Another assumption made by this equation is that the loss of water by infiltration remains negligible under most conditions. Therefore this leaves the main water loss factor as evaporation.

$$Water\ loss = E{\times}Al$$

Applied to steady state conditions, water in=water out.

Therefore: $$Ac{\times}Pf - Al{\times}Pf + Al{\times}P = Al{\times}E$$

$$Ac{\times}Pf = Al{\times}E + Al{\times}Pf - Al{\times}P$$

$$\frac{Ac}{Al} = \frac{E - P}{Pf} + 1$$

This equation is very useful in defining both the hydrologic balance relationship between catchment and lake area and also the climatic parameters affecting the lake. This can be applied to Australian inland as a method of comparing them and characterising which regime they all belong to (figure 12). To convert pan evaporation (E) to a more realistic number for lake surface, a pan conversion factor can be applied of 0.8:

$$Fc = \frac{0.8E - P}{Pf} + 1$$

This function summarises all conditions affecting climatic regimes and therefore can be called the climatic function expression, Fc.
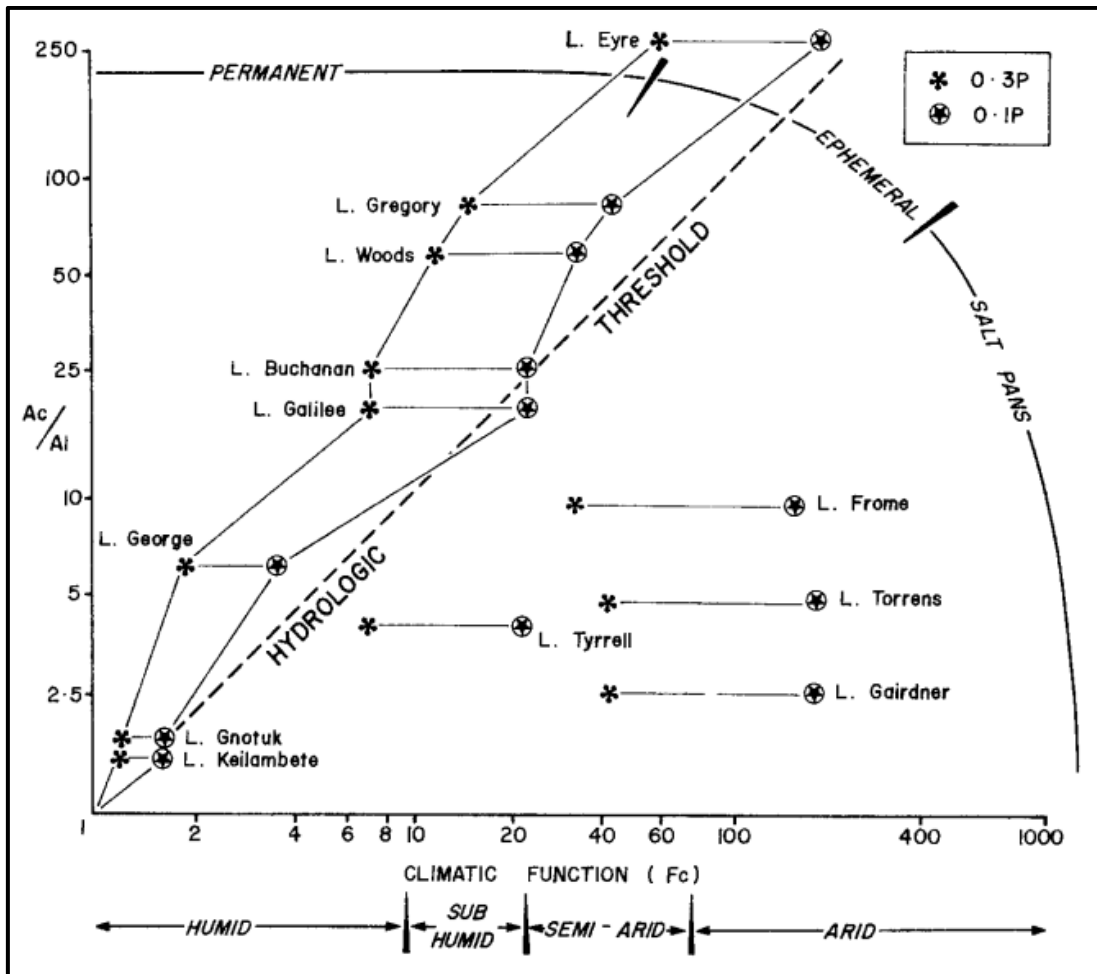
Figure 12 A graph taken from Bowler (1981) comparing inland lakes on a basis of their Fc value. It can be observed from this figure that some lakes, like Lake Torrens, can fall between two climatic regimes depending upon the precipitation index.

The timing of this lake full and lake drying events can be compared to surrounding lakes with previous work done on inland lakes such as Lake Eyre and Lake Callabonna. Magee (2004) found two distinct lake filling events for Lake Eyre in the past 50,000 years and Cohen et al. (2015) found Lake Eyre and Lake Frome had very similar lake levels until approximately 50 ka. However after 50 ka a changed monsoon regime occurred which lead to Lake Eyre and Lake Frome displaying different lake levels throughout the mid to late Holocene (Miller, Magee, Fogel, & Gagan, 2007). Work previously mentioned by Bowler (2003) on Lake Mungo suggests oscillating lake levels since 45ka. The dates collected from the Lake Torrens lunette are maximum 39ka years old and found within a

clay-rich paleosol layer in LTP002. Assuming this clay-rich layer represents a wet phase, this would suggest Lake Torrens has followed a similar climatic regime to Lake Callabonna-Frome than Lake Eyre (figure 13). Lake Torrens and Lake Callabona-Frome indicate a subsequent period of increased rainfall before yet another drying at ~20 ka. This indicates that it was wetter prior to the last Last Glacial Maximum in the inland Australia region, as supported by observed paleosols.

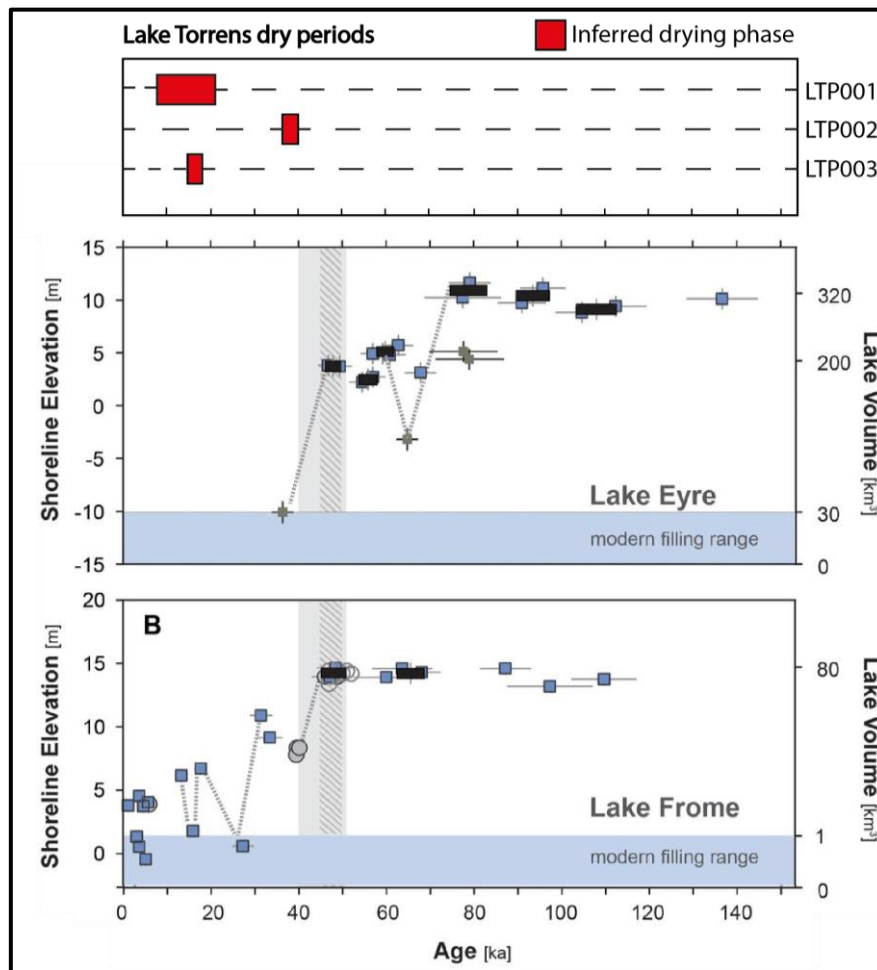**Figure 13** A figure adapted from Cohen et al. (2015) showing the lake level curves of Lake Frome and Lake Eyre based on single grain OSL (blue boxes) and multi grain OSL (black boxes). Most notable is the how lake levels between Frome and Eyre were similar until approximately 50 ka whereas after they diverged with Eyre showing a lower shoreline at 40 ka and Frome showing oscillating lake levels until present.

Lake Torrens vs global sea levels

As mentioned previously, inland lakes are sensitive indicators of global climate. Lakes and surrounding basins distribute a network of catchments able to record physical, chemical and biological responses to climatic changes (Williamson, Saros, Vincent, & Smol, 2009). Inland Australia experienced oscillating periods of wet and dry periods, recorded in lake levels of Lake Frome, Eyre and Torrens. However, the conditions that brought on these oscillations can be observed on a larger scale in global ice volume and global temperatures. These changes are believed to be due to greatly intensified atmospheric circulation aided by increased continental exposure corresponding to glacial low sea levels and reduced seasonal precipitation (J. M. Bowler, 1976). As seen in Figure 14, dates correlating to an arid dry phase interpreted from the lunette sequence studied can be reflected with global temperatures and ice coverage. Arid phases interpreted from this study can correlate to large continental glacial extent, creating a dry and sometimes moist environment, important for paleosol formation.
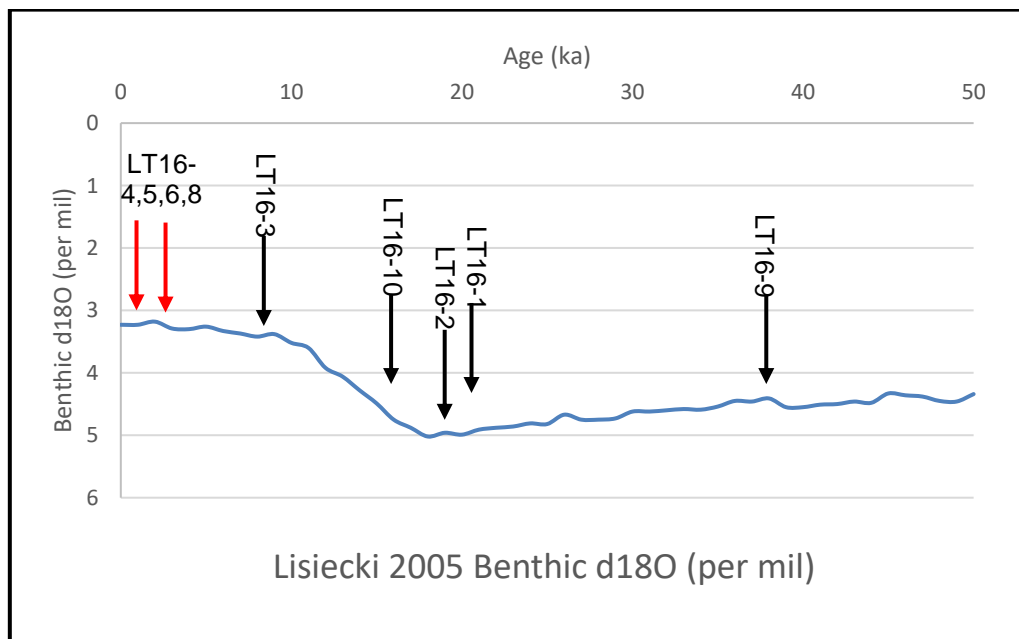

Figure 14 Proxy for global ice coverage up. Dates from a clay rich paleosol layer are displayed using black arrows while dates from sand dominated layers are displayed with red arrows. The orange box

shown overlaying the curve depicts a dry arid phase and the blue box depicts a wet phase as interpreted by the data collected in this study.

What these interpretations made in this study say about the relationship between lake levels of Lake Torrens and global climate is a strong correlation and accurate gauge of climatic settings. The cold arid environment experienced from ~40ka transitions to a humid, wet phase at a minimum age of ~8ka. These soils which can form paleosol root systems also indicate that these periods were stable and had sufficient moisture input and high water table for vegetation growth, as supported by Williams (1973). This also supports the inference put forward by Fitzsimmons (2013) that inland lakes were experiencing arid phases during the time of the Last Glacial Maximum. However the younger ages determined to be from a wet phase also were found in layers which were intermittent with clays, this is also consistent with previous work done of the climate of Holocene inland Australia, suggesting a rapidly changing climatic regime of wet and dry phases.

The lake levels of Australian inland ephemeral lakes also has an impact on megafaunal populations and surrounding ecosystems. As suggested by Miller (2007) Lake Eyre did not receive sufficient enough monsoonal rainfall during the Holocene to establish a permanent deep water lake, which had previously been experienced for longer periods between 130 and 75 ka. This resulting change in climate resulted in a shift of plant life from C_3 to C_4 vegetation as drought tolerant plants encountered more favourable conditions (Johnson et al., 1999). This in turn had an impact on animal life in the surrounding areas which relied on these species of vegetation, with vegetation specific plant herbivores. *Genyornis newtoni,* a small flightless bird which habituated the dunes surrounding Lake Eyre, is one example of extinction pressured by this change in climate

and shift in vegetation. Although it has been shown that dry periods in Lake Eyre have impacted megafaunal populations and the surrounding ecosystems, more study on Lake Torrens needs to be undertaken to conclude if there is evidence to suggest the same patterns have occurred.

CONCLUSIONS

The lunette sequences found throughout the eastern margins of Lake Torrens preserve a vast climate record dating back to at least 40ka. These records suggest that the climate of this region was variable throughout the Quaternary with rapid oscillations between humid and arid phases. However, when consulted with previously published studies, it is clear that these climatic variations were not isolated. The data collected in this study suggests at least two lake drying events has occurred at ~40 ka and ~20ka, with supplement soil formation and vegetation events occurring after these dates. When the lake levels created in this study are then compared to surrounding lakes in the region it was found that Torrens had similar levels to that of Lake Frome. This suggests that Lake Torrens is controlled by a temperate climatic system, however, differences between the Torrens and Frome lake level record could be attributed to the hydrological influences controlling the lakes. On a global scale, Lake Torrens serves as a reliable climatic indicator, supporting isotopic data regarding global glacial extent. It was interpreted that Lake Torrens experienced periods of aridity at ~40 ka and ~20 ka which correlate to large continental glacial ice extent. However more work needs to be performed on Lake Torrens to assess its significance as an indicator of megafaunal populations and ecosystem reconstructions.

ACKNOWLEDGMENTS

REFERENCES

Aitken, M. (1998). An introduction to optical dating : The dating of Quaternary sediments by the use of photon-stimulated luminescence / M.J. Aitken. Oxford ; New York: Oxford University Press.

Bourne, J., & Twidale, C. (2010). Playas of inland Australia. Cadernos do Laboratorio Xeoloxico de Laxe, 2010; 35(35):71-98

Bowler, J. M. (1973). Clay dunes: their occurrence, formation and environmental significance. *Earth-Science Reviews*, *9*(4), 315-338.

Bowler, J. M. (1976). Aridity in Australia: Age, origins and expression in aeolian landforms and sediments. *Earth-Science Reviews, 12*(2), 279-310. doi: http://dx.doi.org/10.1016/0012-8252(76)90008-8

Bowler, J. M. (1981). 30. Australian salt lakes. *Hydrobiologia, 81*(1), 431-444. doi: 10.1007/bf00048730

Bowler, J. M. (1986). Spatial variability and hydrologic evolution of Australian lake basins: Analogue for pleistocene hydrologic change and evaporite formation. *Palaeogeography, Palaeoclimatology, Palaeoecology, 54*(1), 21-41. doi: http://dx.doi.org/10.1016/0031-0182(86)90116-1

Bowler, J. M., & Price, D. M. (1998). Luminescence dates and stratigraphic analyses at Lake Mungo: review and new perspectives. *Archaeology in Oceania, 33*(3), 156-168. doi: 10.1002/j.1834-4453.1998.tb00415.x

Bowler, J. M., Johnston, H., Olley, J. M., Prescott, J. R., Roberts, R. G., Shawcross, W., & Spooner, N. A. (2003). New ages for human occupation and climatic change at Lake Mungo, Australia. *Nature, 421*(6925), 837-840. doi:
http://www.nature.com/nature/journal/v421/n6925/suppinfo/nature01383_S1.html

Campbell, E. M. (1968). Lunettes in southern South Australia. *Transactions of the Royal Society of South Australia*, *92*, 85-109.

Clifton, J., McDonald, P., Plater, A., & Oldfield, F. (1999). An investigation into the efficiency of particle size separation using Stokes' law. *Earth Surface Processes and Landforms, 24*(8), 725-730.

Cohen, T. J., Nanson, G. C., Jansen, J. D., Jones, B. G., Jacobs, Z., Larsen, J. R., . . . Smith, A. M. (2012). Late Quaternary mega-lakes fed by the northern and southern river systems of central Australia: Varying moisture sources and increased continental aridity. *Palaeogeography, Palaeoclimatology, Palaeoecology, 356–357*, 89-108. doi: http://dx.doi.org/10.1016/j.palaeo.2011.06.023

Cohen, T. J., Jansen, J. D., Gliganic, L. A., Larsen, J. R., Nanson, G. C., May, J. H., ... & Price, D. M. (2015). Hydrological transformation coincided with megafaunal extinction in central Australia. *Geology*, *43*(3), 195-198.

De Deckker, P. (1983). Australian salt lakes: their history, chemistry, and biota — a review. *Hydrobiologia, 105*(1), 231-244. doi: 10.1007/bf00025191

Fisher, R. S. (1988). Clay minerals in evaporite host rocks, Palo Duro Basin, Texas Panhandle. *Journal of Sedimentary Research, 58*(5), 836-844. doi: 10.1306/212f8e81-2b24-11d7-8648000102c1865d

Fitzsimmons, K. E., Cohen, T. J., Hesse, P. P., Jansen, J., Nanson, G. C., May, J.-H., . . . Treble, P. (2013). Late Quaternary palaeoenvironmental change in the Australian drylands. *Quaternary Science Reviews, 74*, 78-96. doi: http://dx.doi.org/10.1016/j.quascirev.2012.09.007

Fitzsimmons, K. E., Stern, N., & Murray-Wallace, C. V. (2014). Depositional history and archaeology of the central Lake Mungo lunette, Willandra Lakes, southeast Australia. *Journal of Archaeological Science, 41*, 349-364. doi: http://dx.doi.org/10.1016/j.jas.2013.08.004

Gliganic, L. A., Cohen, T. J., May, J.-H., Jansen, J. D., Nanson, G. C., Dosseto, A., . . . Aubert, M. (2014). Late-Holocene climatic variability indicated by three natural archives in arid southern Australia. *The Holocene, 24*(1), 104-117. doi: 10.1177/0959683613515732

Johns, R. K. (1968). *Investigation of lakes Torrens and Gairdner*. Department of Mines.

Johnson, B. J., Miller, G. H., Fogel, M. L., Magee, J. W., Gagan, M. K., & Chivas, A. R. (1999). 65,000 Years of Vegetation Change in Central Australia and the Australian Summer Monsoon. *Science, 284*(5417), 1150-1152. doi: 10.1126/science.284.5417.1150

Kalita, P. E., Schneider, H., Lipinska, K., Sinogeikin, S., Hemmers, O. A., & Cornelius, A. (2013). High-Pressure Behavior of Mullite: An X-Ray Diffraction Investigation. *Journal of the American Ceramic Society, 96*(5), 1635-1642. doi: 10.1111/jace.12191

Long, D. G. F., McDonald, A. M., Yi Facheng, Li Houjei, Zheng Zili, & Tian Xu. (1997). Palygorskite in Palaeosols from the Miocene Xiacaowan Formation of Jiangsu and Anhui provinces, P.R. China.

Magee, J. W., Miller, G. H., Spooner, N. A., & Questiaux, D. (2004). Continuous 150 k.y. monsoon record from Lake Eyre, Australia: Insolation-forcing implications and unexpected Holocene failure. *Geology, 32*(10), 885-888. doi: 10.1130/g20672.1

McDowell, M. C., Bestland, E. A., Bertuch, F., Ayliffe, L. K., Hellstrom, J. C., Jacobsen, G. E., & Prideaux, G. J. (2013). Chronology, stratigraphy and palaeoenvironmental interpretation of a Late Pleistocene to mid-Holocene cave accumulation on Kangaroo Island, South Australia. *Boreas*, *42*(4), 974-994.

Miller, G. H., Magee, J. W., Fogel, M. L., & Gagan, M. K. (2007). Detecting human impacts on the flora, fauna, and summer monsoon of Pleistocene Australia. *Clim. Past, 3*(3), 463-473. doi: 10.5194/cp-3-463-2007

Ming, S., Chen, G., Wu, Z., Su, L., He, J., Kuang, Y., & Fang, Z. (2016). Effective dispersion of aqueous clay suspension using carboxylated nanofibrillated cellulose as dispersant. *RSC Advances, 6*(44), 37330-37336. doi: 10.1039/C6RA03935A

Quigley, M. C., Sandiford, M., & Cupper, M. L. (2007). Distinguishing tectonic from climatic controls on range-front sedimentation. *Basin Research, 19*(4), 491-505. doi: 10.1111/j.1365-2117.2007.00336.x

Schmid, R. M. (1990). Absolute dating of sedimentation on Lake Torrens with spring deposits, South Australia. *Hydrobiologia, 197*(1), 305-308. doi: 10.1007/bf00026958

Stiles, C. A., Mora, C. I., & Driese, S. G. (2003). Pedogenic processes and domain boundaries in a Vertisol climosequence: evidence from titanium and zirconium distribution and morphology. *Geoderma*, *116*(3), 279-299.

Tsao, T., Chen, Y., Sheu, H., Tzou, Y., Chou, Y., & Wang, M. (2013). Separation and identification of soil nanoparticles by conventional and synchrotron X-ray diffraction. *Applied Clay Science*, *85*, 1-7.

Veth, P., Smith, M., Bowler, J., Fitzsimmons, K., Williams, A., & Hiscock, P. (2009). EXCAVATIONS AT PARNKUPIRTI, LAKE GREGORY, GREAT SANDY DESERT: OSL ages for occupation before the Last Glacial Maximum. *Australian Archaeology*(69), 1-10.

Williams, G. E. (1973). Late Quaternary piedmont sedimentation, soil formation and palaeoclimates in arid South Australia. *Zeitschrift für Geomorphologie*, *17*, 102-125.

Williams, W. D., De Deckker, P., & Shiel, R. J. (1998). The limnology of Lake Torrens, an episodic salt lake of central Australia, with particular reference to unique events in 1989. *Hydrobiologia, 384*(1), 101-110. doi: 10.1023/a:1003207613473

Williamson, C. E., Saros, J. E., Vincent, W. F., & Smol, J. P. (2009). Lakes and reservoirs as sentinels, integrators, and regulators of climate change. *Limnology and Oceanography, 54*(6part2), 2273-2282. doi: 10.4319/lo.2009.54.6_part_2.2273

APPENDIX A: EXTENDED METHODS

Optically Stimulated Luminescence Dating

A total of nine optically stimulated luminescence samples were collected from the 3 different pits and one sample collected from the lake itself with purpose of dating sedimentation events and unit boundaries. Sample collection was carried out by driving PVC piping into the wall of a pit to retrieve the sample itself which was then capped and stored away in light proof bags in an attempt to preserve signal. In situ dose rates were then recorded from the drilled holes where samples were taken to measure the rate of radiative decay. Once returned to the lab each sample was wet sieved into different fractions (>250 µm, 250-212µm, 212-180 µm, 180-125µm, 125-90µm and >90µm) and treated with standard OSL sample preparation procedures, as outlined in Aitken 1998. Once the samples were prepared dose recovery was attempted by on the 250-212µm fraction for each sample using a Risø TL/OSL DA-20 reader. When an equivalent dose was recovered for each sample it was then possible to calculate ages through various spreadsheets based upon the equation given in equation 1.

Equation 1. $$Age = \frac{De\,(gray)}{Dose\,rate\,(\frac{gray}{ka})}$$

Grain Size Analysis

Throughout the lunette sequence three pits with different depths were dug leaving an exposed surface to obtain samples from. Each pit has a narrow sedimentary column collected starting at the surface with samples systematically collected every five centimetres unless a stratigraphic boundary was encountered where a shorter sample was collected to eliminate contamination between units. These samples were then taken to Flinders University to be analysed for grain size distribution using the Mastersizer 2000. Samples were stored in an alfoil tray and dried in a 50ºC oven for approximately 48 hours

with weights being measured before and after drying. Once all moisture was removed, each sample individually was sieved using a 1mm sieve and proportions greater than 1mm weighed, recorded and set aside as the Mastersizer 2000 cannot process grains greater than 1mm in diameter. Individual sample was then added to a 500ml beaker of distilled water until an obscuration range was reached for the Mastersizer settings. Once in range the Mastersizer analysed the grain size distribution by measuring laser diffractions after interacting with individual particles. Once data collection had been completed three beakers of distilled water were run through the machine to best remove and sample remaining in the machine. These results were stored in a linked computer program and exported in an excel spreadsheet once all samples analysed.

X-Ray Diffraction

To obtain a gauge on mineralogical variation through lithologies all samples from the three pits were analysed using x-ray diffraction. To prepare the samples they were crushed to a fine powder using a ring mill then mounted on slides via vibration loading to allow for random orientation of the grains. These prepared discs were placed in an x-ray diffractor and exposed to an x-rays as outlined by (Kalita et al., 2013) for fifteen minutes with all x-ray diffractions recorded being saved in an adjacent computer. From analysing the peaks recorded in the x-ray diffractions it was then possible to identify mineralogical distributions throughout the three pits.

Clay Separation X-Ray Diffraction

To further investigate the mineralogical analysis of the samples collected from the three pits, it was decided that further identification of the clays present was critical to understanding the paleoenvironment at the time of deposition. Six samples were selected based on their position within their pit;

Of these six samples, one gram of each was collected and place into centrifuge tubes and mixed with five ml of CaCl (one mole) for thirty seconds and allowed to rest for thirty minutes.

After thirty minutes the samples were filled with DI water and centrifuged for four minutes at two thousand revolutions per minute to allow for adequate separation.

Once separation was clearly defined each sample was rinsed three times with DI water and filled to ten millimetres with DI water and treated with an ultrasonic probe for one minute at 30% intensity. This energized all the particles in suspension and once the ultrasonic treatment was finished the samples were placed back into the centrifuge for four minutes at nine hundred revolutions per minute, allowing for settling of particles. The target particles were then collected from the middle of the tube within a layer still in suspension, pipetted onto a silica wafer and then left to dry overnight in a 50°C oven. Finally once the samples were dried they were put through the X-Ray diffractor on a much shorter run compared to bulk sample XRD.

Gravimetric distribution analysis

As laser based grain size analysis is still a relatively new technique and sometimes limited in the identification and distinguishing grain sizes it was deemed to be beneficial to perform a proven method to determine grain size. The decision on which samples to be analysed was based upon creating an average grain size for each lithology for each pit (table 1.). To accompany these samples it was also decided to treat the samples that had already undergone clay separation XRD to gauge a more in depth understanding of these specific depths. Ten grams from each sample was taken and treated with one millilitre of sodium tripolyphosphate and five millilitres of sodium hydroxide to act as a clay dispersant. Deionised water was then added to make up volume to one hundred millilitres

and put on an end-over-end shaker for a minimum of sixteen hours. Clay was then decanted into a separate one thousand millilitre beaker, deionised water was then used to make up the volume loss created by the removal of clays. Every sample had the temperature of their contents recorded before being shaken and left for a period of hours dependent on the temperature of the sample, usually the temperature of the water was 18°C which correlated to waiting 8 hours and 25 minutes until sands and silts had settled out of solution.

X-Ray Fluorescence

Obtaining the elemental variation was very significant in complimenting the data retrieved from XRD and further defined unit boundaries already observed in the field. After completing the XRD analysis these samples were then prepared to x-ray fluorescence analysis using a portable XRF reader. Approximately one teaspoon of powdered sediment was taken from each sample and compressed into a small mould and carefully labelled both in preparation and on the built in computer of the scanner. Two lasers were used during measurements, each operating for a minute to determine the amount of energy emitted from individual atoms as these lasers forced a change in their electron configurations. Once the machine was calibrated, three standards were used;

- 1947175 (clay and sand)
- OREAS 901 (argillaceous sandstone)
- 1933084 (carbonate)

Extended Mastersizer Results

Sample	Gravel	Sand	Silt	Clay
LTP001 0-5cm	0.50	84.39	14.07	1.04
LTP001 5-10cm	0.76	77.55	20.52	1.17
LTP001 10-15cm	7.26	66.71	24.59	1.44
LTP001 15-20cm	1.71	75.94	20.84	1.51
LTP001 20-25cm	0.71	73.99	23.34	1.96
LTP001 25-30cm	2.03	61.18	34.25	2.54
LTP001 30-35cm	4.70	69.06	24.53	1.71
LTP001 35-40cm	13.56	57.39	26.84	2.22
LTP001 40-45cm	11.79	57.22	28.91	2.09
LTP001 45-50cm	4.12	58.84	34.23	2.81
LTP001 50-55cm	4.78	63.67	29.41	2.14
LTP001 55-60cm	2.81	65.05	30.16	1.98
LTP001 60-65cm	3.23	68.79	26.31	1.67
LTP001 65-70cm	4.91	69.56	24.23	1.31
LTP001 70-75cm	5.45	70.54	22.82	1.20
LTP001 75-80cm	7.03	70.14	21.64	1.19
LTP001 80-85cm	7.72	65.42	25.03	1.83
LTP001 85-90cm	5.37	64.04	28.26	2.33
LTP001 90-93cm	11.42	54.91	30.85	2.82
LTP001 93-95cm	22.03	49.75	25.70	2.51
LTP001 95-100cm	23.55	56.13	18.21	2.12
LTP001 100-105cm	22.86	63.41	12.29	1.45

Sample	Gravel	Sand	Silt	Clay
LTP002 0-5cm	3.60	92.40	3.75	0.25
LTP002 5-10cm	5.94	89.01	4.51	0.55
LTP002 10-15cm	2.84	90.59	5.89	0.79
LTP002 15-20cm	1.67	92.60	4.94	0.80
LTP002 20-25cm	1.72	90.96	6.41	0.90
LTP002 25-30cm	0.82	93.60	4.82	0.75
LTP002 30-35cm	0.28	91.54	7.00	1.18
LTP002 35-38cm	2.17	91.30	5.72	0.81
LTP002 38-40cm	0.75	93.71	4.96	0.58
LTP002 40-45cm	0.51	92.58	6.26	0.64
LTP002 45-50cm	0.63	95.49	3.65	0.22
LTP002 50-55cm	0.56	96.19	3.25	0.00
LTP002 55-57cm	0.45	95.34	3.95	0.26
LTP002 57-60cm	0.44	93.24	5.23	1.09
LTP002 60-65cm	0.17	92.32	6.14	1.37
LTP002 65-70cm	0.11	93.35	5.18	1.36
LTP002 70-75cm	0.22	94.60	4.14	1.04

Sample	Gravel	Sand	Silt	Clay
LTP002 75-77cm	0.33	93.68	5.01	0.98
LTP002 77-80cm	1.31	88.19	9.72	0.78
LTP002 80-85cm	2.16	86.28	10.91	0.65
LTP002 85-90cm	0.97	84.77	13.58	0.69
LTP002 90-95cm	1.69	79.37	18.06	0.88
LTP002 95-100cm	2.70	72.97	22.96	1.36
LTP002 100-105cm	4.32	61.63	30.97	3.08
LTP002 105-110cm	3.08	62.92	31.09	2.90
LTP002 110-115cm	4.53	65.94	27.51	2.03
LTP002 115-120cm	3.66	67.57	27.21	1.57
LTP002 120-125cm	2.55	72.63	23.72	1.11
LTP002 125-130cm	5.24	70.83	22.96	0.98
LTP002 130-135cm	8.91	70.76	19.60	0.73
LTP002 135-140cm	16.87	64.93	17.53	0.67
LTP002 140-145cm	10.42	70.45	18.42	0.72
LTP002 145-150cm	7.17	73.06	19.02	0.74
LTP002 150-155cm	10.59	68.57	19.81	1.03
LTP002 155-160cm	10.68	66.04	22.14	1.14
LTP002 160-165cm	5.54	78.62	15.10	0.73
LTP002 165-170cm	0.97	85.09	13.18	0.75

Sample	Gravel	Sand	Silt	Clay
LTP003 0-5cm	0.02	84.39	14.77	0.81
LTP003 5-10cm	0.08	85.49	13.48	0.95
LTP003 10-15cm	0.14	85.76	13.16	0.93
LTP003 15-20cm	0.02	88.03	11.14	0.81
LTP003 20-25cm	0.02	88.42	10.84	0.72
LTP003 25-30cm	0.03	85.61	13.68	0.68
LTP003 30-35cm	0.06	92.42	7.05	0.46
LTP003 35-40cm	3.18	88.52	7.70	0.61
LTP003 40-45cm	2.32	89.66	7.41	0.61
LTP003 45-50cm	0.61	90.63	7.70	1.07
LTP003 50-55cm	0.11	89.25	9.68	0.96
LTP003 55-60cm	1.26	89.96	8.09	0.70
LTP003 60-65cm	0.62	92.21	6.60	0.57
LTP003 65-70cm	3.21	90.15	6.13	0.51
LTP003 70-75cm	1.39	91.46	6.43	0.72
LTP003 75-80cm	0.09	92.62	6.57	0.72
LTP003 80-85cm	2.31	88.57	8.34	0.79
LTP003 85-90cm	3.83	85.28	9.59	1.29
LTP003 90-92cm	0.31	94.27	4.58	0.84
LTP003 92-95cm	2.26	75.13	21.36	1.25
LTP003 95-100cm	2.03	74.76	22.21	1.00

LTP003 100-105cm	3.96	69.80	24.65	1.59
LTP003 105-110cm	11.23	64.24	22.05	2.48
LTP003 110-115cm	2.69	71.31	21.92	4.08
LTP003 115-120cm	2.58	71.46	21.26	4.70
LTP003 120-125cm	3.09	68.56	23.74	4.61
LTP003 125-130cm	2.86	62.67	28.55	5.92
LTP003 130-135cm	2.39	74.17	20.83	2.60
LTP003 135-140cm	0.59	73.64	23.07	2.70
LTP003 140-145cm	4.44	63.86	28.40	3.31
LTP003 145-150cm	10.73	51.32	34.15	3.80
LTP003 150-155cm	3.95	65.30	27.48	3.27
LTP003 155-160cm	6.85	66.00	24.55	2.61
LTP003 160-164cm	8.89	65.31	23.27	2.53